Mechanisms of Soybean Roots' Tolerances to Salinity Revealed by Proteomic and Phosphoproteomic Comparisons Between Two Cultivars*[S]

Erxu Pi‡¶¶§§, Liqun Qu‡¶¶, Jianwen Hu§¶¶, Yingying Huang‡¶¶, Lijuan Qiu¶, Hongfei Lu‖, Bo Jiang, Cong Liu‡, Tingting Peng‡, Ying Zhao‡, Huizhong Wang‡, Sau-Na Tsai‡‡, Saiming Ngai‡‡§§, and Liqun Du‡§§**

Understanding molecular mechanisms underlying plant salinity tolerance provides valuable knowledgebase for effective crop improvement through genetic engineering. Current proteomic technologies, which support reliable and high-throughput analyses, have been broadly used for exploring sophisticated molecular networks in plants. In the current study, we compared phosphoproteomic and proteomic changes in roots of different soybean seedlings of a salt-tolerant cultivar (Wenfeng07) and a salt-sensitive cultivar (Union85140) induced by salt stress. The root samples of Wenfeng07 and Union85140 at three-trifoliate stage were collected at 0 h, 0.5 h, 1 h, 4 h, 12 h, 24 h, and 48 h after been treated with 150 mM NaCl. LC-MS/MS based phosphoproteomic analysis of these samples identified a total of 2692 phosphoproteins and 5509 phosphorylation sites. Of these, 2344 phosphoproteins containing 3744 phosphorylation sites were quantitatively analyzed. Our results showed that 1163 phosphorylation sites were differentially phosphorylated in the two compared cultivars. Among them, 10 MYB/MYB transcription factor like proteins were identified with fluctuating phosphorylation modifications at different time points, indicating that their crucial roles in regulating flavonol accumulation might be mediated by phosphorylated modifications. In addition, the protein expression profiles of these two cultivars were compared using LC MS/MS based shotgun proteomic analysis, and expression pattern of all the 89 differentially expressed proteins were independently confirmed by qRT-PCR. Interestingly, the enzymes involved in chalcone metabolic pathway exhibited positive correlations with salt tolerance. We confirmed the functional relevance of *chalcone synthase*, *chalcone isomerase*, and *cytochrome P450 monooxygenase* genes using soybean composites and *Arabidopsis thaliana* mutants, and found that their salt tolerance were positively regulated by *chalcone synthase*, but was negatively regulated by *chalcone isomerase* and *cytochrome P450 monooxygenase*. A novel salt tolerance pathway involving chalcone metabolism, mostly mediated by phosphorylated MYB transcription factors, was proposed based on our findings. (The mass spectrometry raw data are available via ProteomeXchange with identifier PXD002856). ***Molecular & Cellular Proteomics 15: 10.1074/mcp.M115.051961, 266–288, 2016.***

From the ‡College of Life and Environmental Sciences, Hangzhou Normal University, Hangzhou, Zhejiang, 310036, PR China; §Shanghai Applied Protein Technology Co. Ltd, Shanghai, 200233, PR China; ¶The National Key Facility for Crop Gene Resources and Genetic Improvement (NFCRI), Institute of Crop Science, Chinese Academy of Agricultural Sciences, Beijing, P.R. China; ‖College of Life Science, Zhejiang Sci-Tech University, Hangzhou, 310018, PR China; **College of Biology and Food Engineering, Changshu Institute of Technology, Changshu 215500, PR China; ‡‡Centre for Soybean Research of Partner State Key Laboratory of Agrobiotechnology and School of Life Sciences, The Chinese University of Hong Kong, Hong Kong

Received May 18, 2015, and in revised form, September 15, 2015
Published, MCP Papers in Press, September 25, 2015, DOI 10.1074/mcp.M115.051961

Author contributions: E.P. and S.N. designed research; E.P., L. Qu, J.H., Y.H., C.L., T.P., Y.Z., and L.D. performed research; E.P., H.W., and S.N. contributed new reagents or analytic tools; E.P., L. Qu, J.H., Y.H., H.L., B.J., and L.D. analyzed data; E.P., S.T., and S.N. wrote the paper; L. Qiu provide the soybean seed.

Cultivated soybean (*Glycine max* (L.) Merrill) is one of the most important legume crops (1, 2), and is estimated to contributes to 30% of edible vegetable oil and 69% of protein-rich food or feed supplements worldwide (3). However, the yield of soybean is significantly reduced under environmental stresses such as salinity especially during the early vegetative growth stage (3, 4). Soil salinity is estimated to affect at least 20% of the irrigated land worldwide (5, 6) and could affect 50% of the cultivated land by year 2050 (7).

High salinity causes oxidative stress and ionic imbalance in plant cells, and further inhibits the growth and development of the whole plant (6, 8, 9). Elimination of excessive reactive oxygen species (ROS)[1] via glutathione-ascorbate cycle and

[1] The abbreviations used are: ROS, reactive oxygen species; SOS, salt overly sensitive; CDPK, calcium dependent protein kinase; MAPK, mitogen activated protein kinase.

maintaining tolerable salt levels inside the plant cells through exportation or compartmentalization are generally accepted as two major strategies used by plants to survive salinity stress (10). Plants have evolved a series of adaptive mechanisms to sense and respond to salinity cues and these include active involvements of multiple phosphorylation cascades, such as salt overly sensitive (SOS) pathway, phosphatidic acid (PA)-mediated activation of calcium-dependent protein kinase (CDPK), abscisic acid (ABA)-regulated activation of mitogen-activated protein kinase (MAPK) cascades (11–14). Phosphorylation of specific signaling components are known to be initiated at critical time points after plants been subjected to the salt stresses (15) and they coordinate specific metabolic processes, cell-wall porosity and lateral root initiation to help plants adapt to salt stresses (10, 13, 16).

Recently, major high throughput strategies including transcriptomic, proteomic, and metabolomic approaches, have been used to dissect the responses of soybean root to salinity stress (17–21). However, most of these studies were focused on relatively late responses to salinity (*e.g.* over 48 h after Na^+ treatment), earlier signal events minutes after the treatments were apparently ignored. Signaling events through protein phosphorylation are well known to play critical roles mediating appropriate physiological responses in determining the salt-tolerant capability of different soybean species. Many techniques have recently been developed for the specific enrichment of phosphopeptides; these includes immobilized metal affinity chromatography (22), strong cation-exchange chromatography (23, 24), and TiO_2 affinity chromatography (25). The TiO_2 affinity chromatography has been generally accepted as one of the most effective approaches in enrichment of phosphopeptides (26).

Glycine max cultivar Union85140 and *Glycine soja* cultivar Wenfeng07 are salinity sensitive- and tolerant-cultivar, respectively; their drastic difference in salt tolerance enable us to explore the critical proteins contributing the salt tolerance in cultivated soybeans (27, 28). In the present research, we compared the proteomes and phosphoproteomes of these two soybean species at different time points after salinity treatment. Technologies including TiO_2 affinity chromatography, 2-DE MS/MS, and LC-MS/MS were used to generate the row proteome and phosphoproteome data; large-scale bioinformatic analyses including gene ontology (GO) enrichment and phosphorylation motif enrichment were conducted to identified interested targets; functional characterization of selected target genes using gain-of-function composites in soybean and loss-of-function mutant of their homologs in Arabidopsis were conducted to confirm their role in regulating plant tolerance to salt stresses. Our results reveal that normal chalcone metabolism plays a potential role in regulating plant responses to salt stresses in soybean and provide new insights into the mechanism contributing to the difference in salt tolerance of these two soybean cultivars.

EXPERIMENTAL PROCEDURES

Plant Materials and Stress Treatments—Seeds of *Glycine max* cultivar Union85140 (a salt sensitive species) and *Glycine soja* cultivar Wenfeng07 (a salt tolerant species) were kindly provided by Prof. Lijuan Qiu from the Chinese Academy of Agricultural Sciences. The seeds were surface sterilized with 5% NaClO for 5 min and rinsed three times with sterile distilled H_2O. Seeds were germinated in wet filter paper at room temperature (about 22–25 °C) with 40–60% humidity. The seedlings were transferred to 1/4 fold Hoagland's solution. Seedlings at three-trifoliate stage were treated with 150 mM NaCl for 0 h, 0.5 h, 1 h, 4 h, 12 h, 24 h, and 48 h before the root samples were collected for analyses. All the samples were stored at −80 °C until use.

Protein Extraction—Total proteins from roots was extracted as described by Lv et al (29) with minor modifications. Briefly, about 4 g of root tissue for each sample was ground into fine powder in liquid nitrogen. The powder was thoroughly suspended in 45 ml of pre-cooled TCA/Acetone (v:v = 1: 9); the homogenate was settled for overnight and then centrifuged at 14,000 × *g* for 15 min. The pellet was washed three times with acetone and the residual acetone was removed by vacuum. All the above experiments were carried out at 4 °C. 50 mg white powder was resuspended in 800 μl SDT lysis buffer (4% SDS, 100 mM Tris-HCl, 1 mM DTT, 1 mM PMSF, pH7.6, including one-fold PhosSTOP phosphatase inhibitor mixture from Roche), and boiled for 15 min in water bath, and followed by 100 s of sonication. After centrifugation at 14,000 × *g* for 15 min at 4 °C, the protein in supernatant was quantified via BCA (bicinchoninic acid) method (30).

Protein Digestion with Prior Filter Aided Sample Preparation—Approximately 1.5 mg aliquot of dissolved protein for each sample was processed by the filter aided sample preparation method to remove SDS in the samples (31). Briefly, dithiothreitol (DTT) was added to the protein solution to reach 100 mM, and then boiled for 5 min. 25 μl aliquot of each sample was mixed with 200 μl UA buffer (8 M Urea, 150 mM Tris-HCl pH 8.0), loaded into a Microcon filtration devices (Millipore, with a MWCO of 10 kd), and centrifuged at 14,000 × *g* for 15 min; 200 μl of fresh UA buffer was added to dilute the concentrate in the device and centrifuged again. The volume of concentrate was brought to 100 μl with UA buffer supplemented with 50 mM iodoacetamide (IAA) and the sample was shaken at 600 rpm for 1 min. After 30 min incubation at room temperature, the samples were diluted with 40 μl of digestion buffer (contains 5 μg of trypsin). The mixture was shaken at 600 rpm for 1 min, and incubated at 37 °C for 16–18 h. After digestion, the peptide solution was passed through a Microcon filtration device (MWCO 10 kd), and the concentration of the collected peptides was estimated based on their OD at 280 nm (32).

Eight-plex iTRAQ Labeling—For every eight-plex set, a pooled sample was obtained by combing two groups of samples representing seven time points (a control and six salt treatments) from two cultivars (Union 85140 and Wenfeng07). These pooled samples serve as normalizing reference for the peptide content in samples from all the tested eight-plex sets. A 200 μg digested peptides of each sample was subjected to AB Sciex iTRAQ labeling (Fig. 1). The eight-plex iTRAQ labeling was performed according to the manufacturer's instructions. A total of six eight-plex sets of iTRAQ samples were used for the three biological replicates.

Phosphopeptide Enrichment—Phosphopeptides were enriched using TiO_2 beads as described by Ostasiewicz *et al.* (33) with minor changes. Labeled peptide solutions were lyophilized and acidified by dissolving into DHB buffer (3% 2, 5-DiHydroxyBenzoic acid, 80% ACN and 0.1% TFA). The 25 μg of TiO_2 beads (10 μ in diameter, Sangon Biotech) were added to 50 μl peptide solution and spun down after 2 h incubation at room temperature. The pellets were packed into plastic tips (fit to 10 μl pipette), washed 3 times with 20 μl of wash solution 1 (20% acetic acid, 300 mM octanesulfonic acid sodium salt

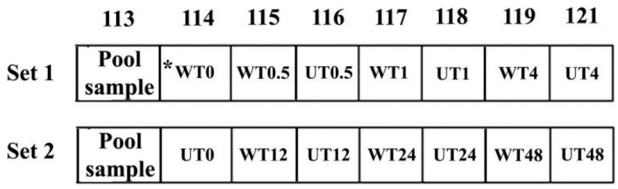

FIG. 1. **Sample set of quantitative phosphoproteomic analysis.** For each biological replication, two eight-plex iTRAQ sets were used for the seven time points (C, T0.5, T2, T4, T12, T24 and T48). A pool sample, combined equally with all the 14 samples, was included in each eight-plex iTRAQ set for normalization between different sets. *W: Wenfeng07; U: Union 85140; T0~T48: Plant treated with 150 mM NaCl for 0 h, 0.5 h, 1 h, 4 h, 12 h, 24 h and 48 h.

and 20 mg/ml DHB) then followed by three times with 20 μl wash solution 2 (70% water; 30% ACN). The enriched phosphopeptides were eluted using freshly prepared ABC buffer (50 mM ammonium phosphate, pH 10.5) and lyophilized for MS analysis.

NanoRPLC-MS/MS Analysis of Phosphorylated Peptides—The lyophilized phosphopeptides were subjected to capillary liquid chromatography tandem mass spectrometry using a two dimensional EASY-nLC1000 system coupled to a Q Exactive Hybrid Quadrupole-Orbitrap Mass Spectrometer (Thermo Scientific). In nanoLC separation system, mobile phase A solution contains 2% acetonitrile (ACN) and 0.1% formic acid in water, and mobile phase B solution contains 84% ACN and 0.1% formic acid. The Thermo EASY SC200 trap column (RP-C18, 3 μm, 100 mm × 75 μm) was pre-equilibrated with mobile phase A before peptides loading. The phosphopeptides were initially transferred to the SC001 column (150 μm × 20 mm, RP-C18) using 0.1% formic acid solution. The peptides were then separated via the trap column using a gradient of 0–55% mobile phase B for 220 min with a flow rate of 250 nL/min followed by a 8 min rinse with 100% of mobile phase B. The trap column was re-equilibrated to the initial conditions for 12 min. The MS data of each sample were acquired for 300–1800 *m/z* at the resolution of 70 k. The 20 most abundant ions from each MS scan were subsequently dissociated by higher energy collisional dissociation (HCD) in alternating data-dependent mode. The HCD generated MS/MS spectra were acquired with a resolution no less than 17,500.

Phosphopeptide Identification and Quantitative Analysis—The raw HCD files were analyzed by Mascot2.2 and Proteome Discoverer1.4 and searched against a peptide database derived from the *Glycine max* genome sequence ("uniprot_Glycine_74305_20140429.fasta" downloaded from http://www.uniprot.org/on April 29, 2014, which includes 74, 305 nonredundant predicted peptide sequences) (34). The Mascot search parameters were list in Table I. The Proteome Discoverer 1.4 was used for integrating the spectra intensity (> 200) of the eight-plex reporter ions. The quantitative value of phosphopeptides at different treatment time points was normalized using the pooled sample as a reference and converted to $\log_2$ value of fold-change. The phosphopeptides pass the cutoff and detected in at least two replicates were used for assessment of significant change in response to NaCl stress. In this research, two statistical approaches were used for significance analysis. The "significance A" value previously described by Cox and Mann (35) was adapted to evaluate the changes between the treated (samples) and untreated (control, T0) root tissues in each biological replicate with each of which includes three technical replicates. A Student's *t* test was performed using the standard deviation of the pooled sample (standard) between different biological replicates for assessing the global variability of all tested samples (29). The phosphopeptides that passed both Significance A < 0.05 and *p* value < 0.05 were considered significantly changed (36).

TABLE I
Parameters of mascot search

Type of search	MS/MS Ion search
Enzyme	Trypsin
Mass values	Monoisotopic
Max missed cleavages	2
Fixed modifications	Carbamidomethyl (C), Itraq8plex(N-term), iTRAQ8plex(K)
Variable modifications	Oxidation (M)
Peptide mass tolerance	± 20 ppm
Fragment mass tolerance	0.1 Da
Protein mass	Unrestricted
Database	Uniprot Glycine.fasta
Database pattern	Decoy
Peptide FDR	≦ 0.01

Protein Shotgun Identifications by Thermo Scientific LTQ Velos—To construct a comprehensive database of salt responsive proteins in soybean, the LTQ Velos Mass Spectrometer coupled to Zorbax 300SB-C18 peptide traps (Agilent Technologies, Wilmington, DE), was used for protein identifications (37). In which, the analytical column is 0.15 mm × 150 mm (RP-C18) (Column Technology Inc., Fremont, CA). Each sample was analyzed three times and the peptides/proteins identified were combined and listed in supplemental Table S1 and S2.

2-DE Gel Based MALDI-TOF/TOF Mass Spectrometer Analysis for Protein Identification—0.2% (w/v) DTT and 0.5% IPG buffer (Lot No.: 17–6000-87, GE Healthcare Life Sciences, Piscataway, NJ) were added into the 200 μg samples before IEF. Total 250 μl samples containing about 200 μg proteins were applied to the dry IPG strips (13 cm, pH 3–10 nonlinear, GE healthcare). The program of IEF was as followed: rehydration at 20 °C for 12 h, 30 V for 8 h, 150 V for 2 h, 500 V for 0.5 h, 1000 V for 0.5 h, 4500 V for 4000 v·hrs, 8000 V for 66000 v·hrs. Focused strips were first equilibrated by incubating in equilibration buffer (pH 8.8, 2% (w:v) SDS, 6 M urea, 50 mM Tris-HCl, 30% glycerol (v:v) containing 1% DTT (w:v) for 15 min, followed by incubation in the abovementioned equilibration buffer containing 4% (w:v) iodoacetamide (IAA) for also 15 min. The second dimension separation was conducted on the 12% acrylamide SDS-PAGE. The PAGE gels were stained with Coomassie brilliant blue for over 2 h. Then, all these gels were captured by magic scanner with the same contrast and brightness. Sequentially, spots in these gel images were analyzed using ImageMasterTM 2D Platinum 5.0 software (GE Healthcare) and their relative volumes (% Vol) were represented as relative abundances. Each sample had at least two independent replicates and the differentially expressed protein spots' relative volumes were compared with Student's *t* test analysis ($p \leq 0.05$). Spots with significant changes were excised out, and destained with 100 μl destaining solution combined with 25 mM ammonium bicarbonate and 50% (v: v) methanol in Milli-Q water. The gel crystals were dehydrated in 100% acetonitrile and vacuum-dried. Then, gel plugs were rehydrated with 10 μg/μl of trypsin in 25 mM ammonium bicarbonate on ice for 40 min and transferred into 30 °C incubator for 16–18 h digestion. Finally, 80% acetonitrile with 20% trifluoroacetic acid (v:v) was used to extracted digested peptides from the gels. MALDI-TOF/TOF mass spectrometer 4700 Proteomics Analyzer (Applied Biosystems, USA) was applied to identify mass spectrometry of digested peptide. The MS scans were acquired among the mass range from *m/z* 700 to 3500 Da and the mass errors were less than 50 ppm. The MS precursor ions corresponding to porcine trypsin autolysis products (*m/z* 805.417, *m/z* 906.505, *m/z* 1153.574, *m/z* 2163.057, and *m/z* 2273.160) were excluded. All MS and MS/MS spectra were search via the MASCOT search engine against the soybean database (source:

http://www.phytozome.net/soybean). The proteins were annotated against Uniprot database. The annotations were confirmed by comparison to the annotation of the top protein hits from the online blast search against the NCBI protein database.

Quantitative RT-PCR Analysis—RNA isolation, mRNA reverse transcription and qRT-PCR methods were performed as described by Wang *et al.* (38) with mini modifications. The root samples were frozen with liquid N_2 and total RNAs were extracted with TRIZOL Reagent (Invitrogen). The genomic DNA was removed with DNase I and cDNA was synthesized using the Plant RNeasy Mini kit (Qiagen) according to the manufacturer's instructions. The primers were generated with NCBI online Primer-BLAST against the *G. max* genome (39). The soybean *actin11* gene was used as a reference for normalization. Quantitative RT-PCR used SYBR™ Premix Ex Taq™ (TaKaRa, Shiga, Japan) and the reaction was conducted on a CFX96 System (Bio-Rad). The gene specific primers are listed in supplemental Table S3.

Bioinformatic Analysis—Peptide motifs were extracted using the motif-X algorithm (40). The width of the generated motifs was set as seven amino acids and serine or threonine was selected as the central amino. Gene oncology (GO) analysis was carried as described by Lv *et al.* (29). The *cis*-elements recognized by transcription factor binding were identified using JASPAR software (41, 42).

Scavenging Activity of the Superoxide Anion (O_2^-) Assay—This assay was based on the method of Zhang *et al.* (43) with slight modifications. Antioxidant enzymes were extracted with 10 ml of 0.05 M phosphate buffer (pH 5.5) from 0.5 g root homogenate. The extract was centrifuged at 12,000 × *g* (4 °C) for 10 min. 1 ml collected supernatant (crude enzyme extract) was added into 4 ml the reaction buffer, which was consist of 2 ml 0.05 M phosphate buffer, 1 ml 0.05 M guaiacol (substrate, overdose) and 1 ml 2% hydrogen peroxide (H_2O_2). The increased absorbance at 470 nm due to the enzyme-dependent guaiacol oxidation was recorded every 30 S until the reaction time reached 4 min. The enzyme's radical scavenging activity (RSA) was defined as: $\text{RSA} = \frac{V_e}{V_t} \times \frac{1}{w} \times \frac{\Delta OD}{\Delta t}$ (g/min), where *w* is the weight of fresh root (*g*), V_t is the volume of crude enzyme used in the reaction mixture (ml), V_e is the total volume of extracted crude enzyme (ml), Δt is the cost time of the reaction (min).

Free Radical Scavenging Activity on ABTS$^{\cdot+}$—The ABTS cationic radical ($ABTS^{\cdot+}$) decolorization assay was done by the method of Re *et al.* (44). $ABTS^{\cdot+}$ working solution was generated by adding 2.45 mM potassium persulphate (final concentration) to 7 mM ABTS (final concentration). This working solution was incubated in dark at room temperature for 12–16 h until it gave an absorbance of 0.70 ± 0.02 at 734 nm. Ten microliters of extracts were mixed with 1.0 ml of working $ABTS^{\cdot+}$ solution and incubated at 30 °C for 30 min and the absorbance of reaction mixture was measured at 734 nm. The enzyme's radical scavenging activity was expressed as: $\text{RSA} = \frac{\Delta OD}{\Delta t} \times \frac{1}{w} \times D_f \times M_0$ (mM/g/min), where ΔOD is the reduced absorbance value, Δt is the reaction time (min), D_f is the dilution factor, *w* is the weight of fresh root (*g*), M_0 is the original $ABTS^{\cdot+}$ concentration.

Na^+ and K^+ Ion Content Analyses—Na^+ and K^+ ion contents were detected followed the methods proposed by Qi *et al.* (45) using the flame atomic absorption spectrophotometer (Shimadzu AA-6300C). The content was expressed as: milligram ion per gram fresh weight (mg/g FW).

Gain-of-function Test of GmCHS, GmCHI, and GmCPM in Soybean Hairy Root System—The full-length CDSs of *GmCHS (Glyma01g43880.1), GmCHI (Glyma04g40030.1), and GmCPM (Glyma07g14460.1*) from Wenfeng07 was cloned into the pCAMBIA1301 vector between NcoI and BglII sites downstream of the ^{35}S promoter. The original pCAMBIA1301 vector was used as a negative control. All these constructs were transformed into the salt-sensitive cultivar Union85140 via agrobacterium rhizogenes strain K599 as previously described (3). The composites were treated in 1/2 fold MS medium with 100 mM NaCl or without NaCl. The seedlings were weighted 10 days after salt treatment.

Loss-of-function Test of AtCHS, AtCHI and AtCPM in Arabidopsis thaliana—The seeds of deletion mutants *chs*, *chs/chi*, *chs/cpm* (Seed stock number: CS85, CS8584, CS8592) were got from ABRC (Arabidopsis Biological Resource Center) and germinated on 1/2 Murashige and Skoog (MS) medium. 5 days after germination, the seedlings were transferred to 1/2 MS medium with or without 150 mM NaCl. The photos of plants were taken 10 days after salt treatment.

RESULTS

Salt stress is well known to cause leaf chlorosis by reducing chlorophyll a, b, and total chlorophyll content (46). After NaCl treatment, we found that the relative contents of chlorophyll a, b, and carotenoids in Union85140 decreased more than that in Wenfeng07 (Fig. 2). In addition, the chlorophyll a/b ratio in Union85140 increased less than that in Wenfeng07 at each time points. These results confirmed that Wenfeng07 is significantly more tolerant to salt stress than Union85140 at the physiological level.

ROS Elimination Capacity and Na^+/K^+ Content in Roots of the Two Soybean Cultivars—The antioxidant property in plant tissue is generally accepted to correlate with plant tolerance to various abiotic stresses including salinity, and it is usually represented by general radical scavenging capacities of peroxidases (POD), ascorbate peroxidase (APX), glutathione S-transferase (GST), and superoxide dismutase (SOD).

The antioxidant properties in salt-treated root tissue of the two cultivars were analyzed using H_2O_2 guaiacol, DPPH (2, 2-diphenyl-1-picrylhydrazyl) and ABTS (2, 2′ -azinobis (3-ethylbenzothiazoline 6-sulfonate)) radical scavenging capacity assays as previously described (47). As shown in Fig. 3*A* and 3*B*, there was no significant difference ($p > 0.05$) between Wenfeng07 and Union 85140 in their superoxide scavenging capacities under normal condition (T0). The scavenging capacities of the superoxide anion (SASA) in these two variants increased consistently at the early stage after salt-treatment (from 1.39 ± 0.03 g^{-1}*min^{-1} in T0 to 4.87 ± 0.12 g^{-1}*min^{-1} at time point T4). Starting from 4th hr (T4) of salt treatment, SASA values in these two cultivars were found to decline from their climaxes. Interestingly, SASA values in the salt-tolerant Wenfeng07 were shown to be higher than that in the salt-sensitive Union 85140 at the first four sampling times after salt treatment (from T0.5 to T12), but declined quicker and to a much lower level than that in Union 85140 24 h after the treatment. Similar to SASA, $ABTS^{\bullet+}$ scavenging potentials in the two tested cultivars displayed peak values at T1 after a short increase, then started to decrease in the rest of the stress treatment. Consistent with their salt tolerance, the $ABTS^{\bullet+}$ scavenging capability of Wenfeng07 were found to be significantly higher than that of Union 85140 ($p < 0.05$) all the time.

In addition, the Na^+ content and Na^+/K^+ ratio were compared in the two cultivars. Our results showed that, changes

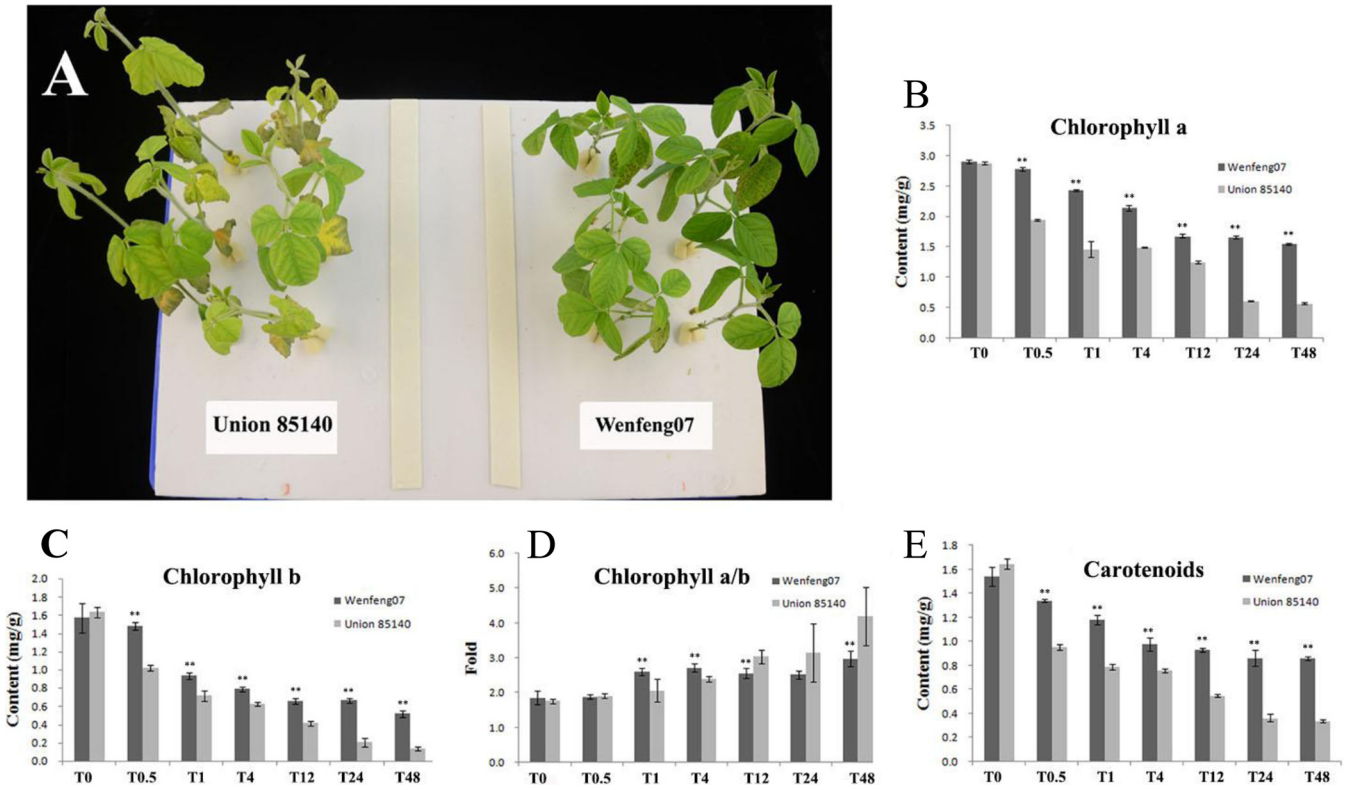

FIG. 2. **Different tolerances of Wenfeng07 and Union85140 to salt stress.** *A*, the cultivar Wenfeng07 showed significant stronger tolerance than Union85140. *B–E*, chlorophyll content analysis. Error bars represent standard error of three biological replicates.

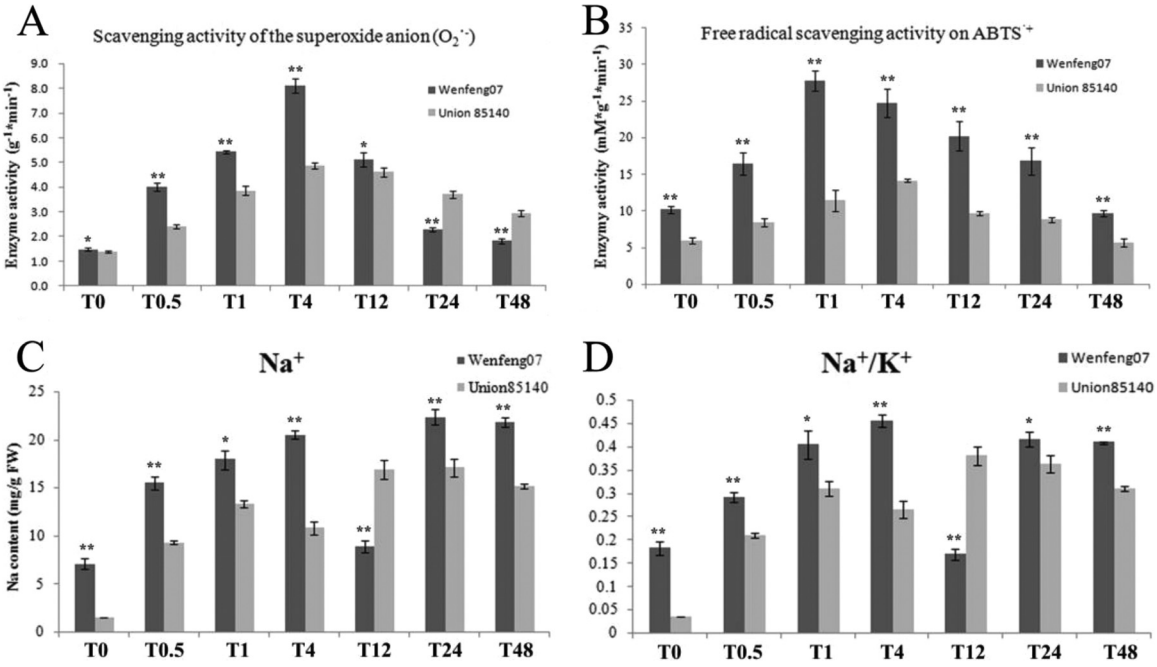

FIG. 3. **Measurement of physiological indices.** *A* and *B*, analysis of ROS scavenger enzymes' activities. *C* and *D*, Na^+ and K^+ relative content analysis (mg per gram fresh wieght). Error bars represent standard error of three biological replicates.

in Na^+ content and the Na^+/K^+ ratio exhibited similar dynamic patterns at different time points in these two cultivars (Fig. 3*C* and 3*D*). The salt tolerant wenfeng07 accumulated higher level of Na^+ (7.0671 ± 0.5495 mg/g FW) than the salt sensitive Union85140 (1.5189 ± 0.0026 mg/g FW) under control condition. The root Na^+/K^+ ratio in wenfeng07 (0.1829 ±

TABLE II
The differential expressed proteins that were identified by LC-MSMS at different time-points

		Control	T0.5	T1	T4	T12	T24	T48
Wenfeng07	Peptides	2526	3209	4020	3610	3306	3394	3140
	Non-redundant peptides	1427	1660	1979	1952	1790	1865	1747
	Non-redundant protein	1854	2055	2217	2146	2199	2115	2116
Union 85140	Peptides	2888	3575	3939	2809	3503	3311	3330
	Non-redundant peptides	1611	1897	2048	1597	1868	1842	1885
	Non-redundant protein	1880	2160	2344	1902	2097	2171	2031

0.0143-fold) was also significantly higher than that in Union85140 (0.0350 $\pm$ 0.0001-fold). After treatment, two peak values of the root Na^+ content were observed at time points T4 and T24 (Fig. 3*C*).

Protein Expression Profiles Revealed by LC-MS/MS—To obtain a comprehensive observation on soybean responses to salinity and to search for clues to the mechanistic differences resulting drastic difference in their tolerance, LC-MS/MS was used to analyze root samples of the two compared species of the soybean subjected to salt stress as described in the previous section. Results of three biological replicates are included in supplemental Tables S1 and S2, and major discoveries are summarized in Table II. A total of 46410 peptides out of 14702 proteins were identified from Wenfeng07 and 46710 peptides out of 14585 proteins from Union85140 (Table II). Of these, 4464 and 4409 nonredundant proteins were found from Wenfeng07 and Union85140 respectively.

In total, there were 89 differential expressed proteins been identified by LC-MSMS between these two cultivars (Table III). In detail, 25 and 20 proteins were specifically detected in Wenfeng07 and Union85140 roots, respectively (Table III). Among the 25 proteins specifically presented in Wenfeng07, many of them including MYB transcription factors (TFs), ethylene-responsive transcription factor 6, chalcone synthase, cytochrome P450 monooxygenase CYP51G1, glutamate receptor and a PDR-like ABC-transporter were previously reported to be related with stress responses (23, 25, 29). Although among the 20 proteins specifically detected in Union85140, the auxin pathway related proteins (such as auxin response factor, auxin-induced protein AUX22 and PIN6a), drought stress responsive protein (KS-type dehydrin SLTI629) and many kinases (such as serine/threonine protein kinase and stress-induced receptor-like kinase 2), might contribute to its general response to salinity stress. Additionally, different homologs of a protein family presented differential expressions in the two varieties. For example, for eukaryotic translation initiation factor 3, the subunit F was expressed with higher abundance in Wenfeng07 roots, whereas the M subunit was expressed with higher abundance in Union85140 roots. Similar dynamics were found in hypersensitive induced reaction protein and nodulin proteins. In addition, the ascorbate peroxidase 2, GST 8, pathogenesis-related protein and two superoxide dismutases (I1LKZ3 and I1LR93) showed opposite trends in these two varieties—they were down-regulated in Wenfeng07, but up-regulated in Union85140.

Transcriptional Expression Analysis of the Salt Responsive Genes—To explore the changes of abovementioned salt responsive proteins at the transcriptional level, 89 primer pairs of the genes encoding these proteins (supplemental Table S3) were synthesized for transcriptional-level analysis via quantitative RT-PCR. Among the 89 differentially expressed proteins, the transcriptional expression patterns of these genes in the salt treatment group were divided into three groups based on their differences between Wenfeng07 and Union85140 (Fig. 4). The first group (28 genes) had higher expression levels in Wenfeng07 than those in Union85140 at most time points, including genes encoding SOD (*Glyma11g19840.2*, *Glyma12g08650.1,* and *Glyma04g39930.1*), serine/threonine protein kinase (*Glyma19g40820.1* and *Glyma20g38980.2*), MYB transcription factor MYB91 (*Glyma07g00930.1*), MYB transcription factor MYB107 (*Glyma08g20270.1*), GST 15 (*Glyma10g33650.1*), and cytochrome P450 monooxygenase (*Glyma07g14460.1*). The second group had lower expression levels in Wenfeng07 at most time points, with 39 genes encoding stress-induced receptor-like kinase (*Glyma15g02450.1*), sterol 24-C methyltransferase (*Glyma04g02271.1* and *Glyma08g19270.1*), Pto kinase interactor (*Glyma02g01150.1*), protein kinase Pti1 (*Glyma10g44212.2*), PR10-like protein (*Glyma05g38110.1*), phosphate transporter (*Glyma19g27380.2*), MYB transcription factor MYB130 (*Glyma01g40220.1*), and hypersensitive induced reaction protein (*Glyma05g01360.3*). The remaining 22 genes were in the third group, among which the gene transcriptional expressions were mostly higher at T1 and T4 in Wenfeng07 but lower at other time points, such as chalcone isomerase (*Glyma06g14820.1* and *Glyma04g40030.1*). Generally, the protein-encoding genes involved in the chalcone metabolism pathway (chalcone synthase, chalcone isomerase, and cytochrome P450 monooxygenase) showed higher expression levels in Wenfeng07. Members of the *GmMYB* TF family were differentially activated in the two cultivars.

2-DE Mapping and Identification of Differentially Expressed Proteins—The 2-DE MS/MS strategy was applied to visualize and quantitatively analyze the defense-related proteins in the roots of two soybean varieties at times T0 and T4. The results showed that 115 protein spots (including 90 nonredundant proteins) of about 900 reproducible spots, demonstrated sig-

TABLE III

The differential expressed proteins that were identified (LC-MSMS) between two variants. Note: "-" indicates no detectable signal been found in sample collected at this (these) time point(s); the amount of "+" shows the number of detectable signal(s) been found in sample collected at this (these) time point(s)

Protein description	Accession No.	Soybean Gene IDs	Wenfeng07		Union 85140	
			Control	Stress	Control	Stress
14-3-3 protein	Q8LJR3	Glyma18g53610.1	−	+	−	−
2-hydroxyisoflavanone dehydratase	Q5NUF3	Glyma01g45020.1	−	+	−	+++++
Alcohol-dehydrogenase	Q9ZT38	Glyma04g41990.1	−	−	−	+
ascorbate peroxidase 1	Q76LA8	Glyma11g15680.5	−	++++++	+	++++++
ascorbate peroxidase 2	Q39843	Glyma12g07780.3	+	−	−	+
Auxin response factor	K7KH37	Glyma03g41920.2	−	−	−	+
Auxin-induced protein AUX22	P13088	Glyma08g22190.1	−	−	−	+
Catalase-1/2	P29756	Glyma17g38140.1	−	++++++	+	+++++
Catalase-3	O48560	Glyma14g39810.1	−	++++	−	+++
Chalcone isomerase 4B	Q53B71	Glyma04g40030.1	−	+	−	+
Chalcone synthase	Q6X0M9	Glyma05g28610.2	−	+	−	−
Chalcone synthase 1	P24826	Glyma08g11620.1	−	+	−	−
Chalcone synthase 2	P17957	Glyma08g11630.2	−	+	−	−
Chalcone synthase 3	P19168	Glyma08g11635.1	−	+	−	−
Chalcone synthase 5	P48406	Glyma01g43880.1	−	+	−	−
Chalcone synthase 7	P30081	Glyma08g11530.1	−	+++	+	+
Chalcone synthase 9	B3F5J6	Glyma08g11610.1	−	+	−	−
Chalcone synthase CHS4	Q6X0N0	Glyma08g11520.1	−	+	−	−
Chalcone-flavonone isomerase family protein	Q6X0M8	Glyma01g22880.1	−	+	−	−
Cytochrome P450 monooxygenase	Q2LAJ9	Glyma07g14460.1	−	+	−	−
Cytochrome P450 monooxygenase	Q2LAL0	Glyma09g05440.1	−	−	−	+
Ethylene-responsive transcription factor 6	C6T283	Glyma12g35550.1	−	+	−	−
Eukaryotic translation initiation factor 3	I1JPD4	Glyma03g32950.5	−	++	−	+++
Eukaryotic translation initiation factor 3	I1JK05	Glyma03g00470.1	−	++	−	++
Eukaryotic translation initiation factor 3	I1JQD9	Glyma03g36470.1	−	+++++	−	++
Eukaryotic translation initiation factor 3	I1M228	Glyma13g31200.1	−	++	−	++
Eukaryotic translation initiation factor 3	C6TC72	Glyma18g03340.1	−	+	−	−
Eukaryotic translation initiation factor 3	I1KXJ9	Glyma08g40110.1	−	+	−	+
Eukaryotic translation initiation factor 3	C6TL4	Glyma12g00510.1	−	+	−	++
Eukaryotic translation initiation factor 3	I1L3W4	Glyma09g29540.1	−	+	−	+
Eukaryotic translation initiation factor 3	I1JUS7	Glyma04g08570.1	−	+	+	+
Eukaryotic translation initiation factor 3	C6TED0	Glyma20g22090.1	−	−	+	+
Ferritin Fer182	I1MYZ9	Glyma18g02800.2	−	−	−	+
Glutamate receptor	I1KFC6	Glyma06g46130.1	−	+	−	−
Glutathione S-transferase GST 15	Q9FQE3	Glyma10g33650.1	−	−	−	+
Glutathione S-transferase GST 24	Q9FQD4	Glyma14g03470.1	−	−	−	++
Glutathione S-transferase GST 8	Q9FQF0	Glyma07g16910.1	+	++	−	+++
Glyceraldehyde-3-phosphate dehydrogenase	Q38IX0	Glyma04g01750.1	−	−	−	++
Heat shock protein 90–2	B6EBD6	Glyma14g01530.1	−	+++++	−	++++
Histone H2A OS	C6SV65	Glyma19g42760.1	+	++++	+	+
Hsp70-Hsp90 organizing protein 1	Q43468	Glyma17g14660.1	−	+	−	+
Hypersensitive induced reaction protein 1	G8FVT3	Glyma19g02370.1	−	−	−	++
Hypersensitive induced reaction protein 3	G8FVT2	Glyma05g01360.3	−	−	+	++
Isoflavone reductase homolog 2	Q9SDZ0	Glyma04g01380.1	−	+++++	+	++++++
KS-type dehydrin SLTI629	A9XE62	Glyma19g29210.1	−	−	−	+
Late-embryogenesis abundant protein 1	C6TLT7	Glyma14g04180.1	−	++++++	+	++++++
Leucine-rich repeat family protein/protein kinase family protein	C6ZRY3	Glyma10g08010.1	−	−	−	++
Lysine–tRNA ligase	I1L9B1	Glyma10g08040.1	−	+	−	−
MATE efflux family protein	I1K9K1	Glyma06g09550.1	−	+	−	−
Mitochondrial phosphate transporter	O80412	Glyma19g27380.2	+	+++++	+	++++++
Mitochondrial Rho GTPase	I1LBC8	Glyma10g29580.1	−	+	−	−
Mitogen-activated protein kinase 2	Q5K6N6	Glyma02g15690.2	−	+	−	+
MYB transcription factor MYB107	Q0PJJ3	Glyma08g20270.1	−	+	−	−
MYB transcription factor MYB130	Q0PJG6	Glyma01g40220.1	−	+	−	−
MYB transcription factor MYB91	Q0PJH2	Glyma07g00930.1	−	+	−	−
NAK-type protein kinase	C6ZRR4	Glyma14g39290.1	−	−	−	+
Nodulin 35	Q9ZWU0	Glyma10g23790.1	−	++	−	−
Nodulin-44	P04672	Glyma13g44100.1	−	−	−	+
Pathogenesis-related protein	C6SZ24	Glyma17g03340.1	+	+++++	+	++++++
PDR-like ABC-transporter	Q1M2R7	Glyma03g32520.1	−	++	−	−
Peroxisomal ascorbate peroxidase	B0M196	Glyma12g03610.1	−	+++	+	+
Phosphate transporter	Q8W198	Glyma19g27380.2	−	++++++	+	++++++

Table III —*continued*

Protein description	Accession No.	Soybean Gene IDs	Wenfeng07		Union 85140	
			Control	Stress	Control	Stress
Phosphatidylinositol-specific phospholipase	Q43439	Glyma02g42430.1	−	+	−	++
Phosphoinositide-specific phospholipase C	Q43443	Glyma14g06450.1	−	+	−	++
PIN6a	M9WP18	Glyma14g27900.1	−	−	−	+
Plamsma membrane-associated AAA-	Q2HZ34	Glyma13g39830.1	+	++	−	++++
Plasma membrane Ca^{2+}-ATPase	Q9FVE7	Glyma06g04900.1	−	+	−	−
PR10-like protein	C6T1G1	Glyma05g38110.1	−	++	+	++++
PR-5 protein	B6ZHC0	Glyma01g42661.1	−	++	+	++
Protein kinase Pti1	C6TCB9	Glyma10g44212.2	−	+++	−	++
Protein ROOT HAIR DEFECTIVE 3	I1KGC2	Glyma07g01230.1	−	+++++	+	++++++
Pti1 kinase-like protein	C6ZRP9	Glyma17g04410.2	−	+	−	−
Pto kinase interactor	C6ZRX5	Glyma02g01150.1	−	−	−	+
Putative chalcone isomerase 4	Q53B72	Glyma06g14820.1	−	++++++	+	++++++
Putative receptor-like protein kinase 2	Q49N12	Glyma13g34100.1	−	+	+	+++++
Serine/threonine protein kinase	C6ZRR6	Glyma19g40820.1	−	+	−	+
Serine/threonine protein kinase	C6ZRT7	Glyma20g38980.2	−	+	−	++
Serine/threonine protein kinase	C6TDV2	Glyma10g01200.1	−	−	−	+
Somatic embryogenesis receptor-like kinase-	C6FF61	Glyma08g19270.1	−	−	−	+
Sterol 24-C methyltransferase 2–1	D2D5G3	Glyma04g02271.1	−	+	−	−
Sterol 24-C methyltransferase 2–2	D2D5G4	Glyma06g02330.1	−	+	−	−
Stress-induced protein SAM22	P26987	Glyma07g37240.2	−	++	+	++++
Stress-induced receptor-like kinase 2	B2ZNZ2	Glyma15g02450.1	−	−	−	+
Superoxide dismutase	I1JYA9	Glyma04g39930.1	−	++	+	++
Superoxide dismutase	I1LCI3	Glyma10g33710.1	−	+++++	+	++
Superoxide dismutase [Cu-Zn]	I1LKZ3	Glyma11g19840.3	+	+++++	−	+++++
Superoxide dismutase [Cu-Zn]	I1LR93	Glyma12g08650.1	+	+++++	−	+++++
Superoxide dismutase [Cu-Zn]	I1LTN6	Glyma12g30260.1	−	++++	−	++++
Superoxide dismutase [Fe], chloroplastic	P28759	Glyma20g33880.2	+	+++++	+	++

nificant changes between T4 and T0 and were successfully identified using MALDI-TOF/TOF-MS (Table IV and V). In particular, 46 differentially expressed proteins were identified from Wenfeng07 and 69 proteins from Union85140 (Fig. 5 and supplemental Fig. S1, Table IV and V).

The results showed that the chalcone flavonone isomerase/chalcone isomerase was also up-regulated in both Wenfeng07 and Union85140, supporting the LC-MS/MS observations. Interestingly, the ascorbate peroxidase 2 (APX2) protein showed two different isoelectric points (Spots 1757 and 1810 in Fig. 5) in Wenfeng07 roots. In addition, Spot 1757 was up-regulated whereas Spot 1810 was down-regulated. Similarly, the stress-induced protein SAM22 and copper amino oxidase proteins also had two different isoelectric points and different mass weights. These two proteins showed opposite down/up change trends after salt treatment in Wenfeng07. In Union85140, the peroxisomal voltage-dependent anion-selective channel protein, fumarylacetoacetase-like, isocitrate dehydrogenase (NADP) (EC 1.1.1.42) and glyceraldehyde-3-phosphate dehydrogenase protein showed three or more spots in the 2-DE gels. Altogether, 14 nonredundant proteins were identified from two or three DEP spots with different isoelectric points and/or molecular weights in the two soybean varieties (Table VI). This implied that the isoforms of the abovementioned proteins might play significant roles in the two varieties.

Phosphopeptide Identification and Quantitative Analysis—The intensity of each phosphopeptide was normalized to the mean of intensities of all phosphopeptides within each biological replicate. Subsequently, the $\log_2$ intensity value changes (salt stress time point Tx/T0) in each condition were calculated for each phosphopeptide (supplemental Table S4). The Student's *t* test (*p* values) was performed using the standard deviation of the pooled sample (standard) between different biological replicates for assessing the global variability of all tested samples (supplemental Table S4).

In total, 5509 phosphorylated sites corresponding to 2692 phosphoproteins were identified (supplemental Tables S4 and S5), and 2344 phosphoproteins containing 3744 phosphorylation sites were quantitatively analyzed. Of these, 34.04% of phosphopeptides were detected in all three biological replicates, and 24.29% in two biological replicates (Fig. S2*A*). In addition, 31.41% of phosphoproteins were detected in all three biological replicates, and 24.97% in two biological replicates (supplemental Fig. S2*B*). Besides, there were 673 protein, which were found by LC-MSMS approaches (supplemental Tables S1 and S2), been also identified as phosphoproteins (supplemental Tables S4 and S5).

Identification of Differentially Expressed Proteins with Phosphorylation Sites—Among the 179 differentially expressed nonredundant proteins (89 nonredundant proteins from LC-MS/MS and 90 nonredundant proteins from 2-DE MS/MS), 16 proteins were also identified as phosphoproteins (Table VII, Fig. 5 and supplemental Fig. S1), such as PIP2,2 (Uniprot accession No. C6TBC3), stress-induced protein SAM22 (Uniprot accession no. Q43453), histone

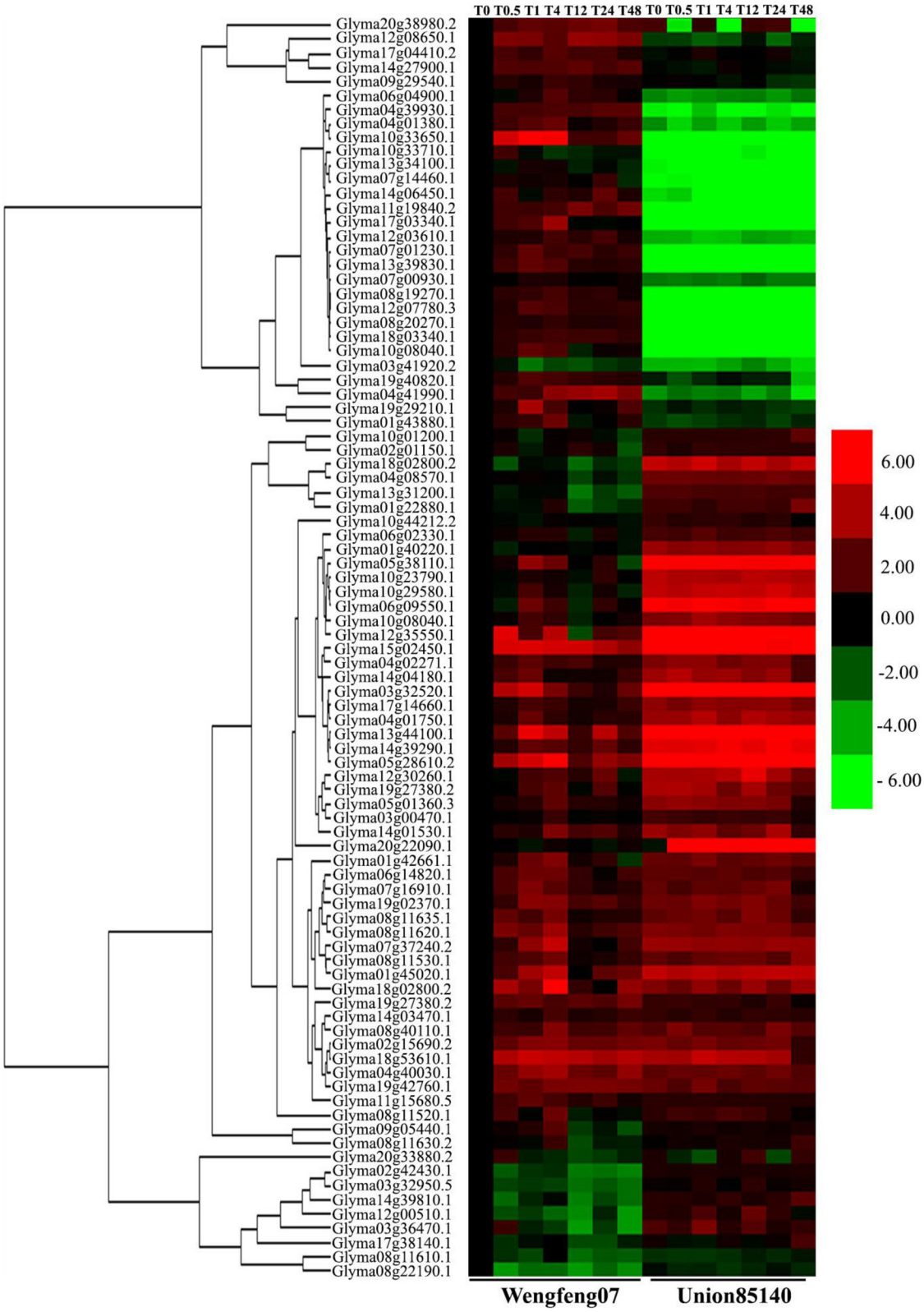

FIG. 4. **Clustering heat map of differentially expressed proteins.** Each column represents a time point of NaCl concentration. The color codes represent the average values of three biological replicates. The abbreviations of gene names were listed in supplemental Table S3.

TABLE IV
Differentially expressed proteins in Wenfeng07 under the salinity stress

Spots No.	Protein No.	Protein description	Theoretial MW/pI	Matched peptide	Protein score	CI%	Changes
675	Glyma10g33680.1	chaperonin CPN60–2, mitochondrial-like isoform 1	61393.4/5.75	15	116	100	Down
3689	Glyma10g39780.7	ubiquitin 11	17168.2/6.75	5	177	100	Down
1342	Glyma13g41960.1	fructokinase-2-like	35375.4/5.29	19	356	100	Down
1304/1394	Glyma04g01380.1	isoflavone reductase homolog 2	33918.7/5.6	14	273	100	Down/down
1528/1561	Glyma09g02800.1	Ferrodoxin NADP oxidoreductase	42241.3/8.38	15	223	100	Down/down
2908/3503/2844	Glyma17g03350.1	stress-induced protein SAM22	16746.6/4.93	13	325	100	Down/up
1320	gi 62546339	PIP2,2	30750.91/8.26	9	230	100	Up
1180	Glyma01g01180.1	malic enzyme/malate dehydrogenase (NADP+)	64985.8/5.83	6	100	100	Up
2170	Glyma03g05480.1	disease resistance response protein 206-like	22015.6/9.88	6	92	100	Up
1466	Glyma03g23890.1	NADP-dependent alkenal double bond reductase P1-like	37896.5/5.94	13	214	100	Up
1819	Glyma03g26060.1	stellacyanin-like	19158.2/5.14	3	68	99.97	Up
1485	Glyma04g16350.2	prohibitin-1, mitochondrial-like isoform 1	30373/7.93	17	231	100	Up
1616	Glyma04g37120.1	elongation factor 1-delta-like	24972.7/4.42	8	190	100	Up
1400	Glyma04g40550.2	nascent polypeptide-associated complex subunit alpha-like protein 2-like	14753.6/5.04	7	236	100	Up
1702	Glyma06g39710.1	proteasome subunit alpha type-6	27366.9/5.58	16	309	100	Up
1493	Glyma06g47520.1	prohibitin-1, mitochondrial-like	30300.9/7.96	18	399	100	Up
1632	Glyma07g33780.1	caffeoyl-CoA O-methyltransferase-like	28053.4/5.46	14	295	100	Up
899	Glyma08g02100.2	monodehydroascorbate reductase, chloroplastic-like	52130.1/8.36	12	169	100	Up
1800	Glyma08g17810.4	proteasome subunit alpha type-2-A-like	25562.2/5.51	12	163	100	Up
1538	Glyma08g24950.1	prohibitin-1, mitochondrial-like	30462.1/7.96	14	148	100	Up
1594	Glyma08g40800.1	mitochondrial outer membrane protein porin of 36 kDa-like	29786.4/7.07	14	219	100	Up
2915	Glyma09g04530.1	ABA-responsive protein ABR17	16522.5/4.68	8	156	100	Up
1916	Glyma09g08340.1	groes chaperonin, putative	26640.2/6.77	18	310	100	Up
1264	Glyma11g33560.1	cytosolic glutamine synthetase GSbeta1	38966.5/5.48	13	274	100	Up
1264	Glyma12g00430.1	putative quinone-oxidoreductase homolog, chloroplastic-like	34810.4/8.27	12	149	100	Up
1820	Glyma12g31850.3	protein usf-like	26332.2/5.38	10	104	100	Up
2112	Glyma13g32300.1	flavoprotein wrbA-like	21653/6.43	10	442	100	Up
285	Glyma13g40130.1	protein disulfide isomerase-like 1–4-like isoform 1	62343.4/4.72	15	165	100	Up
1920	Glyma14g09440.1	cysteine proteinase RD21a-like	50977.4/5.37	11	200	100	Up
1207	Glyma14g36850.1	fructose-bisphosphate aldolase, cytoplasmic isozyme-like	38330/7.12	11	145	100	Up
1610	Glyma14g40670.2	cysteine proteinase 15A-like	40216.1/6.82	8	216	100	Up
1362	Glyma15g15200.1	glucan endo-1,3-beta-glucosidase, basic isoform-like	43758.5/8.75	11	447	100	Up
1928	Glyma15g19970.1	20 kDa chaperonin, chloroplastic-like	26653.2/7.79	10	108	100	Up
370	Glyma16g00410.1	stromal 70 kDa heat shock-related protein, chloroplastic-like	73709.4/5.2	19	230	100	Up
2264	Glyma16g33710.1	Kunitz trypsin protease inhibitor-like precursor	23640.1/5.17	6	172	100	Up
1609	Glyma17g35720.1	cysteine proteinase RD21a-like	52082/5.55	12	413	100	Up
1649	Glyma18g16260.1	mitochondrial outer membrane protein porin of 36 kDa-like	29814.4/7.88	17	254	100	Up
3788	Glyma19g42760.1	Histone H2A OS	14684/10.36	6	329	100	Down
1996	Glyma20g38560.1	chalcone flavonone isomerase	23250.2/6.23	16	432	100	Up
1303/1314	Glyma17g02260.1	copper amino oxidase	75776/6.21	14	147	100	Up/down
1379/1784	Glyma03g28850.1	glucan endo-1,3-beta-glucosidase precursor	38088.3/8.72	18	510	100	Up/up
1380/1393	Glyma05g22180.1	peroxidase 73-like	35475/9.03	12	245	100	Up/up
1539/1941	Glyma09g37570.1	peroxisomal voltage-dependent anion-selective channel protein	29737.6/8.57	14	351	100	Up/Up
1757/1810	Glyma12g07780.2	ascorbate peroxidase 2	27108.8/5.65	15	262	100	Up/Down
1006/1088	Glyma12g32160.1	peroxidase 39-like	35644.1/7.12	9	214	100	Up/Up
2155/2168	Glyma15g41550.1	cytosolic phosphoglycerate kinase	42408.6/5.96	10	103	100	Up/Up

H2A OS (Uniprot accession no. C6SV65), eukaryotic translation initiation factor 3 subunit C (Uniprot accession no. I1JQD9) and glyceraldehyde-3-phosphate dehydrogenase cytosolic-like (Uniprot accession no. I1KC70). These phosphoproteins were involved in signal transduction, chromosome remodeling, gene translation, and energy metabolism (10–14, 29).

Phosphorylation Motif Analysis for Quantitative Phosphopeptides—To extract overrepresented patterns from the 1164 quantitative phosphorylated peptides with differential

TABLE V
Differentially expressed proteins in Union85140 under the salinity stress

Spots No.	Protein ID	Protein description	Theoretial MW/pI	Matched peptide	Protein score	CI%	Changes
796	Glyma02g44080.1	T-complex protein 1 subunit eta-like	60234.2/6.19	9	130	100	Down
988	Glyma03g34830.1	enolase-like	47628.4/5.49	19	473	100	Down
1072	Glyma03g38190.2	S-adenosylmethionine synthase 1-like isoform 1	43196.7/5.57	13	205	100	Down
1221	Glyma04g39380.2	actin-7-like	41688.9/5.31	15	214	100	Down
968	Glyma05g24110.1	elongation factor 1-alpha-like isoform 1	49232.7/9.15	6	54	81.467	Down
910	Glyma05g28490.1	serine hydroxymethyltransferase 2	51686.1/6.9	11	152	100	Down
1217	Glyma05g32220.2	actin-7-like	41711.9/5.37	14	228	100	Down
1216	Glyma06g15520.2	actin-7-like	37069.6/5.38	8	92	99.995	Down
948	Glyma07g30210.1	methylmalonate-semialdehyde dehydrogenase [acylating], mitochondrial-like	57578.5/6.53	15	139	100	Down
699	Glyma07g33570.1	ferredoxin-nitrite reductase, chloroplastic-like	65836.6/6.47	23	271	100	Down
960	Glyma07g36040.1	ferric leghemoglobin reductase-2 precursor	52968.7/6.9	14	152	100	Down
1210	Glyma08g03120.1	biotin carboxylase precursor	58770.2/7.22	20	194	100	Down
892	Glyma08g11490.2	serine hydroxymethyltransferase 2	51733.2/7.59	18	294	100	Down
1154	Glyma08g17490.1	probable inosine-5′-monophosphate dehydrogenase	35562.5/7.68	11	136	100	Down
3400	Glyma08g24760.1	ripening related protein	17750.8/5.96	11	229	100	Down
1486	Glyma08g24950.1	prohibitin-1, mitochondrial-like	30462.1/7.96	14	145	100	Down
1930	Glyma08g40800.1	mitochondrial outer membrane protein porin of 36 kDa-like	29786.4/7.07	13	184	100	Down
951	Glyma10g29600.1	seryl-tRNA synthetase-like	51333.1/6.03	11	76	99.81	Down
2302	Glyma11g07540.1	Transcription factor APFI-like protein	29247.9/6.36	10	119	100	Down
1334	Glyma11g08920.1	isocitrate dehydrogenase	39315.3/6.47	11	140	100	Down
1106	Glyma1337s00200.1	S-adenosylmethionine synthase-like	43027.7/5.65	17	391	100	Down
2011	Glyma13g01040.2	Mitochondrial outer membrane protein porin	29738.2/8.66	9	87	99.984	Down
2222	Glyma13g32300.2	flavoprotein wrbA-like	21112.7/6.09	7	66	98.052	Down
574	Glyma13g41370.1	protein TOC75–3, chloroplastic-like	87454/7.29	22	236	100	Down
1263/2324/2388	Glyma13g41960.1	fructokinase 2	35375.4/5.29	17	272	100	Down
1032	Glyma14g02530.3	dihydrolipoyllysine-residue succinyltransferase component of 2-oxoglutarate dehydrogenase complex 2, mitochondrial-like	50131.5/9.17	10	128	100	Down
3449	Glyma15g13140.1	actin-depolymerizing factor 2-like	10414.2/5.65	6	215	100	Down
1113	Glyma15g21890.2	S-adenosylmethionine synthase-like isoform 1	43025.8/5.5	22	472	100	Down
3191	Glyma15g31520.1	ripening related protein	21494.8/6.29	10	148	100	Down
929	Glyma17g04210.1	dihydrolipoyl dehydrogenase, mitochondrial-like	52854.5/6.9	13	148	100	Down
531	Glyma17g35890.1	polyadenylate-binding protein 2-like	71880/5.7	12	120	100	Down
1694	Glyma17g37050.1	proteasome subunit alpha type-1-A-like isoform 1	30956.4/5.07	12	183	100	Down
1983	Glyma18g16260.1	mitochondrial outer membrane protein porin of 36 kDa-like	29814.4/7.88	16	264	100	Down
973	Glyma19g37520.1	enolase	47643.4/5.4	20	507	100	Down
439	Glyma20g19980.1	chaperonin CPN60–2, mitochondrial-like isoform 1	60983.3/6.38	12	83	99.965	Down
1087	Glyma20g38030.1	26S protease regulatory subunit 6A homolog A-like	47425.4/4.98	23	331	100	Down
1527/1535/1544/1877/2814	Glyma09g37570.1	peroxisomal voltage-dependent anion-selective channel protein	29737.6/8.57	11	320	100	Down/up/down/down/up
1229	Glyma02g46380.2	pyruvate dehydrogenase E1 component subunit beta, mitochondrial-like	38696.8/5.7	11	127	100	Up
3364	Glyma03g05480.1	disease resistance response protein 206-like	22015.6/9.88	7	122	100	Up
1402	Glyma03g23890.1	NADP-dependent alkenal double bond reductase P1-like	37896.5/5.94	11	249	100	Up
3112	Glyma03g38630.1	germin-like protein 1	22832.2/9.06	5	180	100	Up
675	Glyma04g01220.1	phosphatidylinositol transfer-like protein III	70795.2/8.44	12	57	83.799	Up
2219/2293	Glyma04g01380.1	isoflavone reductase homolog 2	33918.7/5.6	16	347	100	Up
2436	Glyma05g22180.1	peroxidase 73-like	35475/9.03	10	229	100	Up
3481	Glyma05g38160.1	Protein yrdA, putative	27715.5/8.34	12	157	100	Up
1151	Glyma06g12780.3	alcohol dehydrogenase 1-like	36891.4/5.77	16	357	100	Up
2158	Glyma07g33780.1	caffeoyl-CoA O-methyltransferase-like	28053.4/5.46	10	140	100	Up
3103	Glyma07g37250.2	Stress-induced protein SAM22	15524.9/4.74	8	228	100	Up
3319	Glyma08g17810.4	proteasome subunit alpha type-2-A-like	25562.2/5.51	11	216	100	Up
788	Glyma09g40690.1	2,3-bisphosphoglycerate-independent phosphoglycerate mutase	60831/5.51	7	182	100	Up
697	Glyma10g41330.2	ATP synthase subunit beta, mitochondrial-like	58664.8/8.83	18	479	100	Up

Table V —*continued*

Spots No.	Protein ID	Protein description	Theoretial MW/pI	Matched peptide	Protein score	CI%	Changes
1438	Glyma11g07490.1	isoflavone reductase homolog A622-like	33978.9/6.12	12	187	100	Up
1160	Glyma11g33560.1	cytosolic glutamine synthetase GSbeta1	38966.5/5.48	11	194	100	Up
1978	Glyma11g34380.2	tropinone reductase homolog At1g07440	29159.8/7.56	9	164	100	Up
3362	Glyma12g31850.3	protein usf-like	26332.2/5.38	6	74	99.731	Up
3914	Glyma13g32300.1	flavoprotein wrbA-like	21653/6.43	8	325	100	Up
2478	Glyma14g36850.1	fructose-bisphosphate aldolase, cytoplasmic isozyme-like	38330/7.12	14	201	100	Up
3217	Glyma15g04290.1	triosephosphate isomerase, cytosolic-like	27181.1/5.87	16	494	100	Up
1874	Glyma15g13550.1	peroxidase C3-like isoform 1	38103.7/8.62	6	108	100	Up
2301	Glyma15g13680.1	Ferredoxin–NADP reductase, root isozyme, chloroplastic	42164.3/8.52	12	174	100	Up
2334	Glyma15g15200.1	glucan endo-1,3-beta-glucosidase, basic isoform-like	43758.5/8.75	13	468	100	Up
1936	Glyma15g27660.1	alpha-amylase/subtilisin inhibitor-like isoform 1	23521.5/4.77	9	137	100	Up
2171	Glyma17g10880.3	malate dehydrogenase, chloroplastic-like	43120.4/8.11	11	185	100	Up
2109	Glyma17g15690.1	expansin-like B1-like	27650.4/6.3	7	229	100	Up
3672	Glyma20g38560.1	chalcone flavonone isomerase	23250.2/6.23	16	456	100	Up
1218/1388	Glyma12g32160.1	peroxidase precursor	35644.1/7.12	13	226	100	Up/up
969/970/1276	Glyma09g01270.2	fumarylacetoacetase-like	40512.1/6.49	14	197	100	Up/Up/down
3199/3208	Glyma02g40820.1	isocitrate dehydrogenase (NADP) (EC 1.1.1.42)	46050.5/5.87	18	156	100	Up/up/up
1979/1983/2133	Glyma06g18110.7	Glyceraldehyde-3-phosphate dehydrogenase	36662/8.30	3	199	100	Up/up/up

changes between the two cultivars, the software MEME Suite and motif-X were used to analyze the motifs generated at different time points after salinity treatment from the two soybean cultivars. The intensities of phosphopeptides from Wenfeng07 (I_{pW}) were compared with those from Union85140 (I_{pU}) and the ratio values (I_{pW}:I_{pU}) with significant (p value $<$ 0.05) differences were divided into two groups. When the intensity value $I_{pW} > I_{pU}$, its corresponding phosphopeptide was categorized into the Up group, whereas the phosphopeptide with $I_{pW} < I_{pU}$ was categorized into the Down group. The Up group represented the peptides with higher phosphorylation level in the salt-tolerant cultivar and lower phosphorylation level in the salt-sensitive cultivar. There were ten phosphorylation motifs enriched from the Up group (Fig. 6*A*) and 14 motifs enriched from the Down group (Fig. 6*B*). In addition, Ser and Thr were observed as the central phosphorylated amino acid residue in both groups, with much higher frequency for Ser. In both the Up and Down groups, the amino acid closely neighboring the phosphorylated Ser/Thr was mainly Pro or Asp (Fig. 6). There were six phosphorylation motifs ([sP], [xDsDx], [xsxxD], [xsxSx], [xsxDx], and [Sxxsx]) enriched from both Up and Down groups. Four motifs ([xsxPx], [xsDxE], [xsxEx], and [Pt]) were only found in the Up group, and eight ([xPxsPx], [xDsx], [xsxDD], [xsSPx], [Dxxsx], [Axxsx], [xtPx], and [xtDx]) only in the Down group. These differentially regulated motifs were then searched for their target kinases in relevant databases, for example, [sP] is a potential substrate of plant MAPK and [sDxE] is recognized by casein kinase-II (29, 48, 49).

The Phosphorylated TFs and Their Specific Binding Motif in Enzymes Involved in Chalcone Metabolism—Several transcription factors, including MYB, bZIP, WRKY, ERF, BTF and GTE families were identified with fluctuating phosphorylation modifications at different time points of salt treatment (supplemental Tables S4 and S5). For example, ten GmMYB family proteins were quantitatively analyzed on one or more phosphorylated peptides. Interestingly, the phosphorylated peptide TVPSAsG in GmMYB I1KQI5 was detected in both cultivars, and another phosphorylated peptide FsPNLNQNPNPNLGK could only be detected in Union85140 (supplemental Tables S4 and S5), indicating that phosphorylation of the same protein could be modified at different sites in the two cultivars and might generate various activations. In addition, the phosphorylated peptide QKIDDsDESPNPK in GmMYB K7MQI8 in both cultivars was only detected at late time points (T12-T48) (supplemental Table S4). Similar results were observed in GmMYBs (K7LAB8 and I1JE71), GmbZIPs (Q00M78, I1JDF7, K7MV95, and C6T6L1), GmWRKY (I1MT25) and GmERF (I1KN17). This suggested a temporary regulation of this modification in response to salt stress.

To reveal the potential interaction network between TFs and differentially expressed proteins, the TF-specific binding motifs of the promoters from enzymes involved in chalcone metabolism are summarized in Fig. 7. Motif structures of these promoters were retrieved from the JASPAR database (50). All the promoters of genes encoding chalcone synthase (*GmCHS*), chalcone isomerase (*GmCHI*), and cytochrome P450 monooxygenase (*GmCMP*) were predicted to contain the conserved motifs recognized by MYBs, indicating that the promoters of these 13 enzymes should be regulated by this TF family. In addition, promoters of the two *GmCMP* and one *GmCHI* also included motifs recognized by bZIP. Additionally, GmERF had potential binding motifs in promoters of some *GmCHS*, *GmCMP* and *GmCHI* genes. Because their activities might be regulated by phosphorylation modifications, these

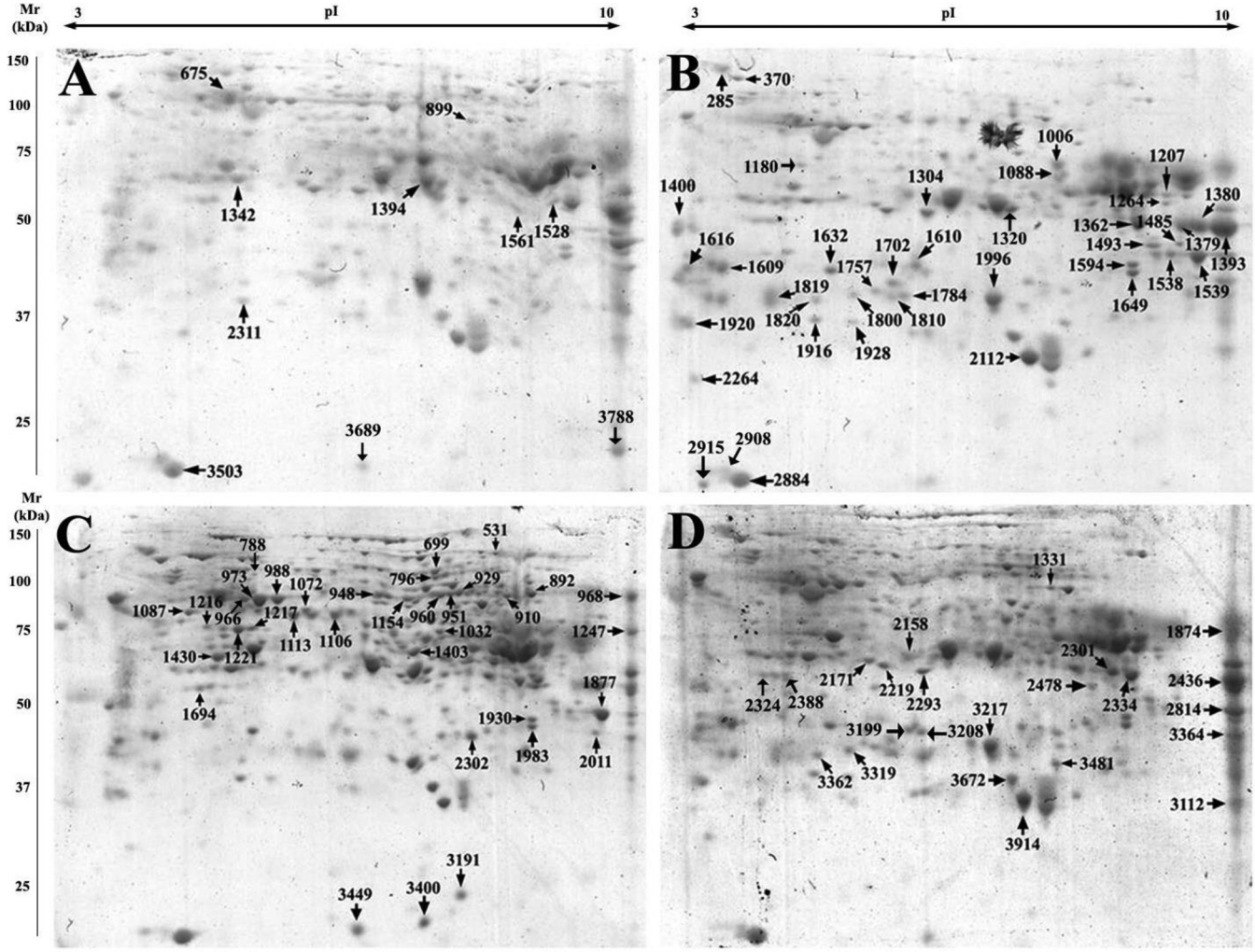

FIG. 5. **Different expressed proteins in Wenfeng07 and Union85140 identified by 2-D MS/MS under salinity stress (at time points T0 and T4).** SDS-PAGE gels were stained with Coomassie Brilliant Blue; *A* and *B*, 2-D maps of root proteome of Wenfeng07 at time points T0 and T4, respectively; *C* and *D*, 2-D maps of root proteome of Union85140 at time points T0 and T4, respectively.

TABLE VI

*Differential expressed proteins identified with two or more spots on 2-DE gels. *W: Wenfeng07; U: Union 85140*

Uniprot accession No.	Protein description	IDs on 2D gel	Theoretial MW/pI
Q9ZNZ6	peroxidase precursor	1218/1388	35644.1/7.12
I1LU76	peroxidase 39-like	1006/1088	35644.1/7.12
I1MRA7	copper amino oxidase; diamine oxidase	1303/1314	75776/6.21
I1MJC7	cytosolic phosphoglycerate kinase	2155/2168	42408.6/5.96
C6T8Y4	Ferrodoxin NADP oxidoreductase	1528/1561	42241.3/8.38
I1M561	fructokinase 2	1263/2324/2388	35375.4/5.29
I1KZY9	fumarylacetoacetase-like	969/970	40512.1/6.49
C6TL98	glucan endo-1,3-beta-glucosidase precursor	1379/1784	38088.3/8.72
C6T857	isocitrate dehydrogenase (NADP) (EC1.1.1.42)	3199/3208	46050.5/5.87
Q9SDZ0	isoflavone reductase homolog 2	2219/2293	33918.7/5.6
Q39843	L-ascorbate peroxidase 2	1757/1810	27108.8/5.65
C6THQ0	peroxidase 73-like	1380/1393	35475/9.03
I1L602	peroxisomal voltage-dependent anion-selective channel protein	1527/1535/1544/1539/1877/1941/2814	29737.6/8.57
Q43453	stress-induced protein SAM22	2908/3503	16746.6/4.93

TABLE VII
Differential expressed proteins identified with reliable phosphorylated sites

Protein No.	Uniprot accession No.	Protein description	Phosphorylated peptide	Phosphorylated site (probabilities)
Glyma09g40690.1	I1L6W0	2,3-bisphosphoglycerate-independent phosphoglycerate mutase	AHGTAVGLPTEDDMGNSEVGHNALGAGR/ AHGTAVGLPTEDDMGNSEVGHNALGAGR	T(4): 0.0; T(10): 0.0; S(17): 100.0/T(4): 0.0; T(10): 95.9; S(17): 4.1
Glyma01g45020.1	Q5NUF3	2-hydroxyisoflavanone dehydratase	LLSSENVAASPEDPQTGVSSK	S(3): 0.0; S(4): 0.0; S(10): 100.0; T(16): 0.0; S(19): 0.0; S(20): 0.0
Glyma06g12780.3	C6TD82	alcohol dehydrogenase 1-like	IIGVDLVSSR	S(8): 100.0; S(9): 0.0
Glyma11g33560.1	C6TJN5	cytosolic glutamine synthetase GSbeta1	WNYDGSSTGQAPGEDSEVIIYPQAIFR	Y(3): 0.0; S(6): 33.3; S(7): 33.3; T(8): 33.3; S(16): 0.0; Y(21): 0.0
Glyma11g33560.1	C6TJN5	cytosolic glutamine synthetase GSbeta1	WNYDGSSTGQAPGEDSEVIIYPQAIFR	Y(3): 0.0; S(6): 33.3; S(7): 33.3; T(8): 33.3; S(16): 0.0; Y(21): 0.0
Glyma04g37120.1	C6SXP1	elongation factor 1-delta-like	AAVAEDDDDDDVDLFGEETEEEK	T(19): 100.0
Glyma03g36470.1	I1JQD9	eukaryotic translation initiation factor 3 subunit C	YFVDNASDSDDSDGQK/SDSEASQYDNEK	Y(1): 0.0; S(7): 100.0; S(9): 100.0; S(12): 100.0/S(1): 100.0; S(3): 0.0; S(6): 0.0; Y(8): 0.0
Glyma14g36850.1	C6TMG1	fructose-bisphosphate aldolase, cytoplasmic isozyme-like	LASISVENVESNR/LADGASESLHVEDYK/GILAADESTGTIGK	S(3): 98.5; S(5): 1.5; S(11): 0.0/S(6): 0.1; S(8): 99.9; Y(14): 0.0/S(8): 98.3; T(9): 1.7; T(11): 0.0
Glyma06g18110.7	I1KC70	glyceraldehyde-3-phosphate dehydrogenase, cytosolic-like	EASYDEIK	S(3): 98.9; Y(4): 1.1
Glyma19g42760.1	C6SV65	histone H2A OS	GEIGSASQEF	S(5): 0.0; S(7): 100.0
Glyma19g29210.1	A9XE62	KS-type dehydrin SLTI629	EHGHEHGHDSSSSSDSD/EHGHEHGHDSSSSSDSD/ EHGHEHGHDSSSSSDSD	S(10): 32.9; S(11): 32.9; S(12): 32.9; S(13): 0.6; S(14): 0.6; S(16): 0.0/S(10): 91.0; S(11): 8.3; S(12): 4.5; S(13): 0.5; S(14): 4.7; S(16): 91.0/S(10): 0.5; S(11): 0.5; S(12): 67.0; S(13): 67.0; S(14): 67.0; S(16): 98.1
Glyma10g08010.1	C6ZRY3	leucine-rich repeat family protein/protein kinase family protein	EEDFSYSGIFPSTR/SSELNPFANWEQNTNSGTAPQLK	S(5): 0.0; Y(6): 0.0; S(7): 0.0; S(12): 98.3; T(13): 1.7/S(1): 0.0; S(2): 0.0; T(14): 33.3; S(16): 33.3; T(18): 33.3
Glyma01g01180.3	I1J4J8	malic enzyme OS	IWLVDSK	S(6): 100.0
Glyma14g39290.1	C6ZRR4	NAK-type protein kinase	VQSPNALVIHPR	S(3): 100.0
gi 62546339	C6TBC3	PIP2,2	DVEQVTEQGEYSAK	T(6): 0.0; Y(11): 1.1; S(12): 98.9
Glyma17g03350.1	Q43453	stress-induced protein SAM22	SVENLEGNGGPGTIK	S(1): 100.0; T(13): 0.0

FIG. 6. **Phosphorylation motifs enriched from sequence of peptide with different modification levels in two cultivars.** *A*, phosphorylation motifs extracted from the phosphopeptides in the Up group by motif-X. *B*, phosphorylation motifs extracted from the phosphopeptides in the Down group by motif-X.

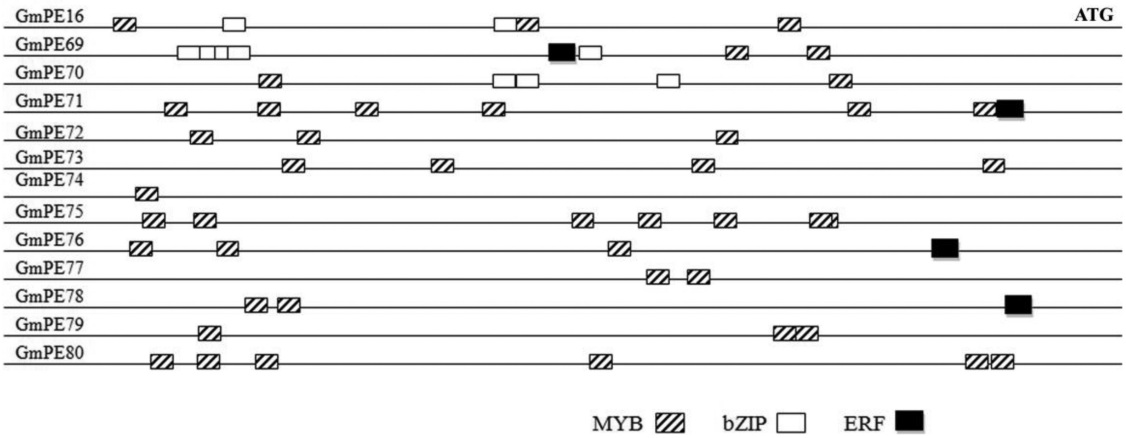

FIG. 7. **TFs specific binding motifs in promoters of *GmCHS*, *GmCHI* and *GmCMP* genes in soybean.** All the promoters (2000 bp) of tested genes were scanned for discovering conserved motifs recognized by MYB, bZip and ERF TFs (88% threshold) at JASPAR (http://jaspar.genereg.net/cgi-bin/jaspar_db.pl?rm=browse&db=core&tax_group=plants). The abbreviations of gene names were listed in supplemental Table S3.

TFs should play significant roles in the bridge between stress signal and the transcription of salt responsive genes.

Rapid Function Tests of the Genes Involved in Chalcone Metabolism—In this research, the enzymes involved in chalcone metabolism were proposed to have potential correlations with soybean salt tolerance at both proteomic and transcriptional levels. To further validate that the chalcone synthase (CHS), chalcone isomerase (CHI) and cytochrome P450 monooxygenase (CPM) were determinants of plant salt-tolerance, gain-of-function and loss-of-function analyses were tested in soybean composites (Fig. 8) and *A. thaliana* mutants (Fig. 9), respectively, at seedling stage.

When subjected to NaCl treatments, the Union85140/*gmchs*-ox composites showed higher tolerance than Union85140/pCAMBIA1301 (negative control) (Fig. 8), indicating that chalcone was a positive regulating factor in salt tolerance. Both of the gain-of-function Union85140/*gmchi*-ox and Union85140/*gmcpm*-ox composites (Fig. 8) showed a slight lower tolerance than the negative control. Similar results were observed in Arabidopsis, the single deletion mutant (*chs*) showed significantly lower tolerance than wild type (Fig. 9*A* and 9*B*), indicating that chalcone was a positive regulating factor in salt tolerance. Both of the loss-of-function double mutants *chs*/*cpm* (Fig. 9*C* and 9*D*) and *chs*/*chi* (Fig. 9*E* and 9*F*) also showed lower tolerance than wild type. However, these double mutants (*chs*/*cpm* and *chs*/*chi*) showed higher tolerance than the single deletion mutant (*chs*), suggesting that chalcone isomerase and cytochrome P450 monooxygenase were two negative regulating factors in salt tolerance. To summarize, chalcone synthase dominated the response to salt stress in chalcone metabolism.

DISCUSSION

Compared with the salt-sensitive Union85140, the salt-tolerant Wenfeng07 showed no significant advantage in exportation or compartmentalization of salts, but much higher capacity for ROS elimination within 48 h of NaCl treatment. Plants have evolved very complex mechanisms for ROS elimination at the transcription, translation and post-translational modification levels (12, 13, 15, 29, 51). The present study involved a comparative analysis of salt stress responses between a salt-tolerant and a salt-sensitive soybean variety using proteomic and phosphoproteomic approaches. Among them, 89 representative differentially expressed proteins were checked with their changes at transcriptional level using quantitative RT-PCR. Our results confirmed the view that expression differences at proteomic level are involved in functional proteins, whereas differences at phosphoproteomic level are mainly related to regulatory proteins (29). Interestingly, a series of proteins related to ROS scavenging and protein folding/degradation—such as GST, APX, SOD, heat shock protein 90–2, and Hsp70-Hsp90 organizing protein 1—were involved in salt responses of both salt-tolerant and salt-sensitive varieties, which were almost in accordance with previous studies (17, 52, 53). However, tolerance discriminations were possibly dominated by: (1) synthesis of flavonoid/isoflavonoid involved in the salicylic acid defense pathway by chalcone metabolism (54, 55) in Wenfeng07, compared with initiation of lateral roots by auxin response factor, auxin-induced protein AUX22 and PIN6a (10) in Union85140; (2) up-regulation of ERF and MYB TFs for activating MAPK and SOS pathways to eliminate ROS and excessive salts (12, 13) in Wenfeng07; and (3) regulating innate immunity via cytochrome P450 monooxygenase, chalcone isomerase, and sterol 24-C methyltransferase (56, 57) specifically in Wenfeng07.

However, phosphoproteomic comparisons revealed the details of dissimilarities in stress signal perception and transduction, transcription/translation of response genes and protein transporting. The protein samples were analyzed based on 2-DE MS/MS and LC MS/MS proteomics. A total of 89 differentially expressed nonredundant proteins were identified

FIG. 8. **Effects of salinity stress on seedlings of soybean composites.** The seedlings of negative control (Union85140/pCAMBIA1301), *gmchs*-ox (Union85140/*GmCHS*), *gmchi*-ox (Union85140/*GmCHI*) and *gmcpm*-ox ((Union85140/*GmCPM*)) composites were treated in 1/2 MS medium with or without 100 mM NaCl for 10 days. Bar: 1 cm.

in LC MS/MS analysis and 90 in 2-DE MS/MS analysis. Of the 179 nonredundant differentially expressed proteins from LC-MS/MS and 2-DE MS/MS, 16 were also identified as phosphoproteins, including the stress-induced protein SAM22, histone H2A OS, eukaryotic translation initiation factor 3 subunit C, elongation factor 1-delta-like, fructose-bisphosphate aldolase, cytosolic glutamine synthetase GSbeta1 for signal transduction, chromosome remodeling, gene translation, energy and small molecular metabolism, etc.

Perception of Salinity and Signal Transduction—The SOS system (e.g. SOS1: H9CDQ2, supplemental Table S4) acts as a central hub in preventing Na^+ toxicity in the plant, especially for Wenfeng07. The most common role of the SOS system is to sequestrate Na^+ ions from the plant cytosol (58). In general, the high salt stress suddenly triggers a cytosolic Ca^{2+} signature (59), which can be perceived by the calcineurin B-like protein, SOS3 and Ser/Thr protein kinase, SOS2 (60). After perceiving the Ca^{2+} signature, SOS3 is phosphorylated by the protein kinase SOS2. The SOS2/SOS3 complex activates the plasma membrane Na^+/H^+ antiporter, SOS1. Downstream of the SOS cascade, SOS1 mediates Na^+ efflux at the root epidermis (61). In our study, there were many SOS2 and SOS3 homologs found with multiphosphorylated sites and with different regulation levels. For example, GmSOS2 (K7KTI3) was observed with four phosphorylation sites, in which phosphor-Ser in peptide LPEsPREGSEEDNFLENLTGMPIR only occurred at early time points T0.5-T4, but the phosphor-Ser in peptide EGsEEDNFLENLTGMPIR only occurred at late time points T12-T48 (supplemental Table S4). Interestingly, GmSOS3 (C6T458), both in Wenfeng07 and Union85140, was detected at T0 and all treatment times except T4 (supplemental Table S4). In addition, another GmSOS3 homolog

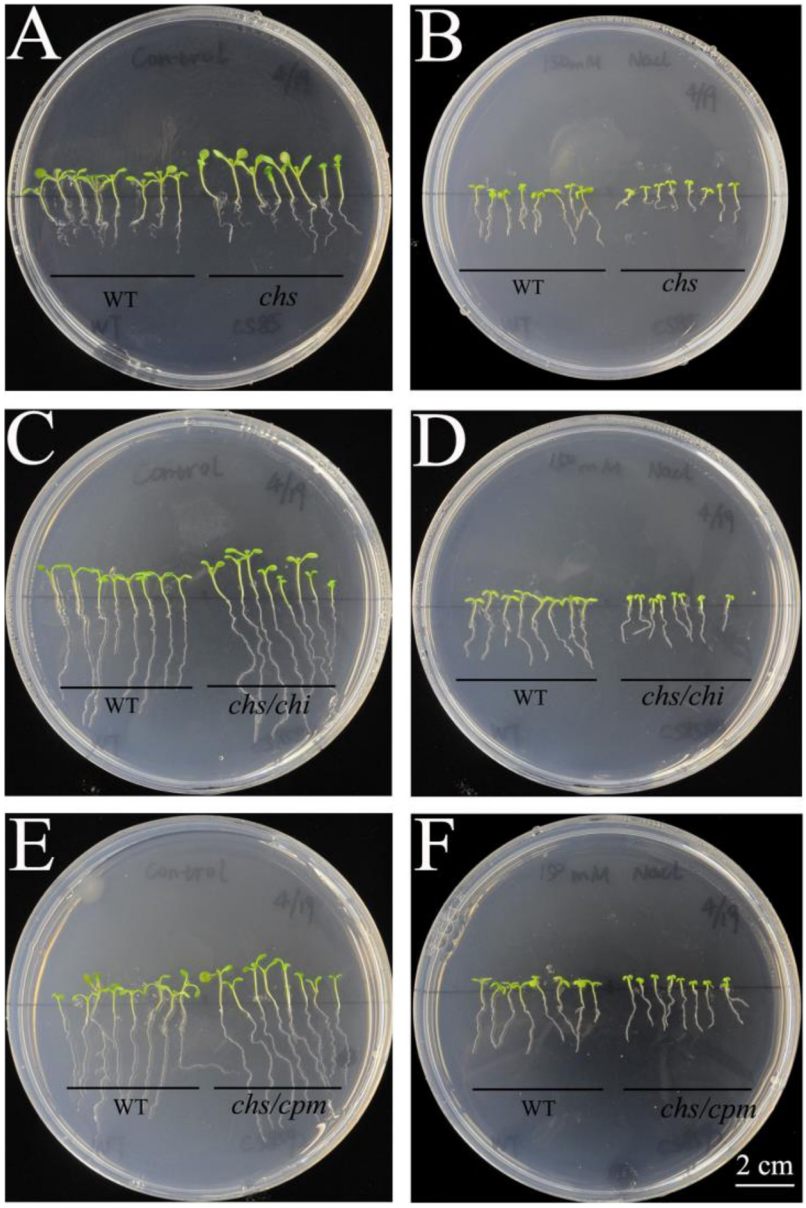

FIG. 9. **Effects of salinity stress on seedlings of *Arabidopsis thaliana* mutants.** The germination of Col-0 (WT), *chs*, *chs*/*chi* and *chs*/*cpm* plants grown in 1/2 Murashige and Skoog (MS) medium for 5 days and then transferred to 1/2 MS medium with or without 150 mM NaCl for 10 days. *A* and *B*, comparison of salt tolerance between WT and deletion mutant *chs*. *C* and *D*, comparison of salt tolerance between WT and double deletion mutant *chs*/*chi*. *E* and *F*: comparison of salt tolerance between WT and double deletion mutant *chs*/*cpm*. A, C, E: 0 mM NaCl; B, D, F: 150 mM NaCl; Bar: 2 cm.

(K7KLX6), from both cultivars, was detected at time points T12-T48.

The Ca^{2+} signature could also be perceived by calcium-dependent protein kinases (CDPKs or CPKs) (62). The latter two transmit the signal into phosphorylation cascades capable of modulating gene expression and target protein activity (63). CDPKs, through their interaction with ion channels and transporters, seem to represent part of membrane-delimited plant stress responses (64). In the present study, the GmCDPK (D3G9M7) in Wenfeng07 showed much higher phosphorylation levels than Union85140 for time points T0.5-T48 (supplemental Table S4). This suggested that this GmCDPK might significantly contribute to the salt tolerance of Wenfeng07.

Reactive oxygen species (ROS) and hormones are key elements in intricate switches used by plants to trigger highly dynamic responses to changing environment. Although ROS may have deleterious effects in cells, they also act as signal transduction molecules involved in mediating responses to environmental stresses (65). Plant plasticity in response to the environment is linked to a complex signaling module in which ROS and antioxidants operate together with hormones, including auxin (66). The auxin resistant double-mutant *tir1 afb2* showed increased tolerance to salinity as measured by chlorophyll content, germination rate and root elongation. In addition, mutant plants displayed reduced hydrogen peroxide (H_2O_2) and superoxide anion ($O_2^{\cdot -}$) levels, as well as enhanced antioxidant metabolism (67). Microarray analyses in-

dicated that auxin responsive genes are repressed by oxidative and salt treatments in rice (68). More recently, the transcriptomic data of Blomster *et al.* (69) showed that various aspects of auxin homeostasis and signaling are modified by apoplastic ROS. Together, these findings suggest that the suppression of auxin signaling might be a strategy of plants to enhance their tolerance to abiotic stress, including salinity. In this study, the auxin response factor K7M7H1 was found with phosphorylated serine (in peptide sPPQPR). However, this modification was only detected at late time points T12-T48 (supplemental Table S4). Recent research found that a salt-responsive ethylene response factor1 (ERF1) regulates ROS-dependent signaling during the initial response to salt stress (13). However, the GmERF (I1KN17) was only observed with phosphorylation modification in the sensitive cultivar Union85140 (supplemental Table S4).

Other reported pathways of salt signaling include mitogen-activated protein kinase (MAPK or MPK) cascades (70). A MAPK cascade consists of a MAPK kinase (MAPKkk)–MAPK kinase (MAPKK/MKK)–MAPK module that links salt-signal receptors to downstream targets (71). For a rapid signal transduction, the GmMAPKK2 (Uniprot accession no. Q5JCL0) showed a much higher level phosphorylation modification after NaCl treatment in both Wenfeng07 and Union85140 (supplemental Table S4).

Metabolism of Small Molecules Related to Detoxification and Defense Pathways—Under salinity stress, the plant employs detoxification and defense pathways to increase their tolerance (58). Several abiotic stresses, such as salt, drought and cold can induce ROS accumulation including $O_2^{\cdot -}$, H_2O_2 and hydroxyl radicals (10). Suitable concentrations of ROS are acquired as substrates in lipid, sugar and protein metabolisms. Peak values of ROS concentration usually act as signals for inducing ROS scavengers, which are mainly substrates involved in these metabolisms. In this study, copper amino oxidase and quinone oxidoreductase, which produces ROS (72, 73), were up-regulated after salt treatment. Meanwhile, universal scavengers, such as APX, SOD, GST and POD, also showed up-regulation in roots of both salt-sensitive and -tolerant soybean. Among these scavengers, APX has been shown to reduce H_2O_2 to H_2O, with the concomitant generation of monodehydroascorbate. Many reports demonstrating that APX overexpression can enhance the salt tolerance of different plants have confirmed that APX plays an important role in scavenging ROS produced by salinity stress (74–77). Moreover, the two homologs of APX might have different efficiencies in ROS elimination, because APX2 was significantly up-regulated in the tolerant cultivar (Wenfeng07), whereas APX1 was significantly up-regulated in the sensitive cultivar (Union85140) after salt treatment. This result is consistent with findings in two rice APXs (78).

Chalcone Metabolism Pathway is Involved in Soybean Tolerance to Salt Stress—Up to now, the chalcone metabolism pathway has mainly been considered as a feasible strategy for enhancing plant immunity to microbes (79–81). In plants, chalcone biosynthesis begins with the hydroxylation of cinnamic acid by cytochrome P450 monooxygenase (82). The intermediate product p-coumaric acid is then activated by 4-coumaroyl:CoA ligase, yielding p-coumaroyl-coenzyme A (CoA) (83, 84). Subsequently, malonyl-CoA is added to p-coumaroyl-CoA and yields tetrahydroxychalcone by the enzyme chalcone synthase. Finally, chalcone isomerase converts the C15 compound tetrahydroxychalcone into (2S)-flavanones (85–87). These flavonoids, including a diverse family of polyphenols, have been proven with health-promoting effects especially in preventing various human pathological risks (88, 89). Hence, significant amounts of research have been stimulated to elucidate the biosynthetic networks of flavonoids (90, 91). However, there are very few reports on the contribution of chalcone metabolism to plant salt tolerance (92, 93). Recently, a cytochrome P450 monooxygenase mutant was shown to be involved in a series of abiotic stresses including ABA and salt in Arabidopsis (94). Our proteomic and phosphoproteomic analyses showed that key enzymes, such as cytochrome P450 monooxygenase, chalcone synthase and chalcone isomerase, were correlated with salt stress especially in tolerant cultivar Wenfeng07. Their salt-responsive dynamics were also confirmed at the transcriptional level. The functions of these enzymes were preliminarily tested in soybean composites and Arabidopsis mutants. Both the gain of function and loss-of-function tests demonstrated that cytochrome P450 monooxygenase and chalcone isomerase were negatively related with salt tolerance in plant seedlings, whereas chalcone synthase was positively related.

Interestingly, 10 MYB (MYB like) transcription factors (TFs) were identified with significantly changed phosphorylation sites (supplemental Table S4 and S5). Commonly, MYB TFs play crucial roles in flavonol accumulation by regulating the expression of series genes coding for key enzymes involved in chalcone metabolism in plants (95–97). In addition, three chalcone metabolism enzymes have been found in response to salt stress. These results indicate that the network between phosphorylated MYB TFs and chalcone metabolism enzymes might play potential crucial roles in soybean's tolerance to salinity.

CONCLUSION

Plants have evolved a set of physiological and biochemical responses for adaptation to salinity stress. Generally, glutathione and proline as well as several secondary metabolites, such as flavonoids, play a pivotal role in tolerance/detoxification of plants (98–100).

In the present research, quantitative proteomic and phosphoproteomic analyses were conducted with both salt-tolerant (Wenfeng07) and -sensitive (Union85140) soybean varieties under salt stress. LC-MSMS and 2-D gel based proteomic analysis of these two variants from a series of time points after salt treatment identified 179 differentially expressed nonre-

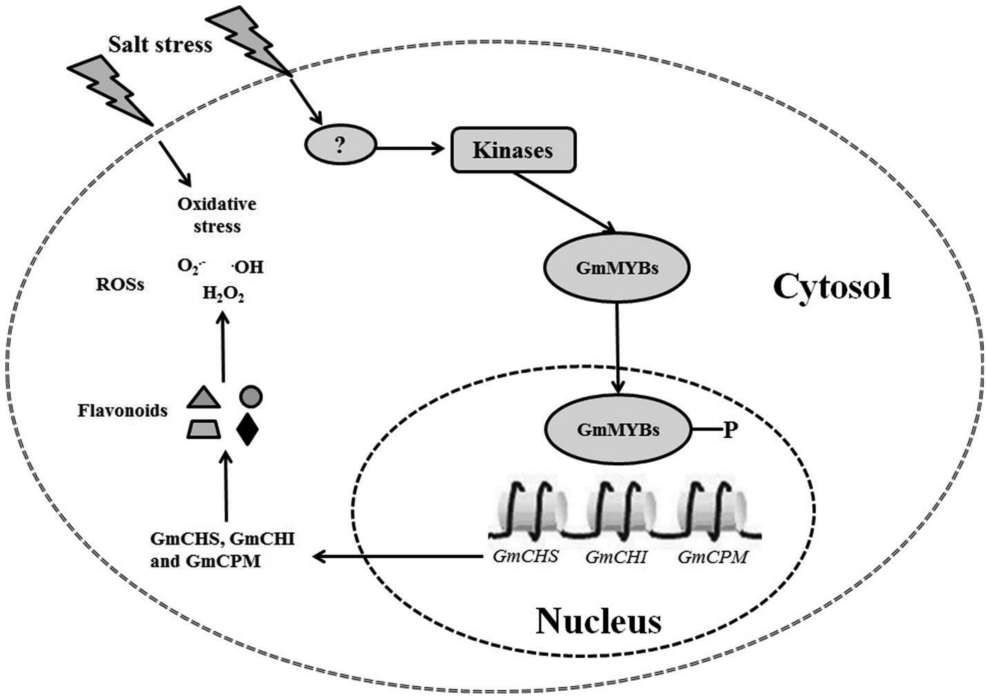

FIG. 10. **A hypothetical model for transcription factor GmMYB in regulating genes *GmCHS*, *GmCHI* and *GmCPM* during soybean's response to salinity.** After the perception of salinity signal, the GmMYBs are phosphorylated and further activated the genes *GmCHS*, *GmCHI* and *GmCPM*. Then, these key enzymes GMCHS, GmCHI and GmCPM regulated the accumulation patterns of flavonoids. Finally, these flavonoids appropriately reduced the ROS or play roles in other functions for soybean's tolerance to salinity.

dundant proteins in total. Of these, 16 proteins also showed changes at phosphorylation level. These differential protein expression characteristics were mostly involved in functional pathways which possibly dominated the capacity of the two varieties concerning salt tolerance.

The quantitative phosphoproteomic analysis identified 3744 phosphorylated sites and 1163 differentially changed sites between the two cultivars, which revealed an activated signaling cascade involved in salt response. The comparison at phosphorylation level indicated that the hub signals fitted with salt tolerance in the tolerant variety.

In summary, the proteomic and phosphoproteomic comparisons between tolerant and sensitive variants could aid understanding of the response and defense mechanisms of soybean in response to salinity stress. The transcriptional and functional analyses confirmed the correlation of significantly changed proteins with salt tolerance. Moreover, the identified significantly changed proteins and phosphorylated sites provide an array of potential salt-response markers for future work. More importantly, the chalcone metabolism pathway was shown as a likely novel candidate for further research on plant salt tolerance. Based on these findings, we hypothesized a novel soybean salinity-tolerance pathway involved in chalcone metabolism (Fig. 10). After the perception of salinity signal, the GmMYBs are phosphorylated and further activated the genes *GmCHS*, *GmCHI* and *GmCPM*. Then, these activated key enzymes GMCHS, GmCHI and GmCPM mediated the accumulation patterns of flavonoids. Finally, these flavonoids appropriately reduced the ROS or play roles in other functions for enhancing the soybean's tolerance to salinity.

Acknowledgments—We thank Prof. Rencun Jin, Prof. Weiqin Zhu, Miss Yanqin Gu and M_r Zhengzhe Zhang, from Hangzhou Normal University, for their kind assistance during the ion content analysis. Special appreciations should also be paid to Dr. Rui Wang and Dr. Xiaojing Gao, from Shanghai Applied Protein Technology Co. Ltd., for their kind help for bioinformatics analysis. The mass spectrometry proteomics data have been deposited to the ProteomeXchange Consortium via the PRIDE partner repository with the dataset identifier PXD002856.

* This work was partially supported by grants 31301053 and U1130304 from the National Science Foundation of China, the Hong Kong RGC Collaborative Research Fund (CUHK3/CRF/11G), the Hong Kong RGC General Research Fund (468610), the Lo Kwee-Seong Biomedical Research Fund and Lee Hysan Foundation, and grant PF14002004014 from Hangzhou Normal University.

S This article contains supplemental material.

§§ To whom correspondences should be addressed: Hangzhou Normal University, Xuelin Street No. 16, Xiasha, Hangzhou 310018, China. Tel.: 86-571-28865199; E-mail: pierzaixian001@aliyun.com (E. P.) or liqundu@hznu.edu.cn (L.D.), or to Centre for Soybean Research of Partner State Key Laboratory of Agrobiotechnology and School of Life Sciences, The Chinese University of Hong Kong, Shatin, NT, Hong Kong SAR, China. Tel.: 852–39436025; E-mail: smngai@cuhk.edu.hk (S.N.).

¶¶ These authors contributed equally to this work.

REFERENCES

1. Berman, K. H., Harrigan, G. G., Riordan, S. G., Nemeth, M. A., Hanson, C., Smith, M., Sorbet, R., Zhu, E., and Ridley, W. P. (2009) Compositions of

seed, forage, and processed fractions from insect-protected soybean MON 87701 are equivalent to those of conventional soybean. *J. Agr. Food Chem.* **57,** 11360–11369
2. Prakash, D., Niranjan, A., Tewari, S. K., and Pushpangadan, P. (2001) Underutilised legumes: potential sources for low-cost protein. *Int. J. Food Sci. Nutr.* **52,** 337–341
3. Lam, H. M., Xu, X., Liu, X., Chen, W., Yang, G., Wong, F. L., Li, M. W., He, W., Qin, N., Wang, B., Li, J., Jian, M., Wang, J., Shao, G., Wang, J., Sun, S. S., and Zhang, G. (2010) Resequencing of 31 wild and cultivated soybean genomes identifies patterns of genetic diversity and selection. *Nat. Genet.* **42,** 1053–1059
4. Li, W. Y., Shao, G., and Lam, H. M. (2008) Ectopic expression of GmPAP3 alleviates oxidative damage caused by salinity and osmotic stresses. *New Phyt.* **178,** 80–91
5. Yamaguchi, T., and Blumwald, E. (2005) Developing salt-tolerant crop plants: challenges and opportunities. *Trends Plant Sci.* **10,** 615–620
6. Munns, R., and Tester, M. (2008) Mechanisms of salinity tolerance. *Annu. Rev. Plant Biol.* **59,** 651–681
7. Wang, W., Vinocur, B., and Altman, A. (2003) Plant responses to drought, salinity and extreme temperatures: towards genetic engineering for stress tolerance. *Planta* **218,** 1–14
8. Kim, B. G., Waadt, R., Cheong, Y. H., Pandey, G. K., Dominguez-Solis, J. R., Schultke, S., Lee, S. C., Kudla, J., and Luan, S. (2007) The calcium sensor CBL10 mediates salt tolerance by regulating ion homeostasis in Arabidopsis. *Plant J.* **52,** 473–484
9. Ward, J. M., Hirschi, K. D., and Sze, H. (2003) Plants pass the salt. *Trends Plant Sci.* **8,** 200–201
10. Galvan-Ampudia, C. S., and Testerink, C. (2011) Salt stress signals shape the plant root. *Curr. Opin. Plant Biol.* **14,** 296–302
11. Osakabe, Y., Yamaguchi-Shinozaki, K., Shinozaki, K., and Tran, L. S. P. (2013) Sensing the environment: key roles of membrane-localized kinases in plant perception and response to abiotic stress. *J. Exp. Bot.* **64,** 445–458
12. Yu, L. J., Nie, J. N., Cao, C. Y., Jin, Y. K., Yan, M., Wang, F. Z., Liu, J., Xiao, Y., Liang, Y. H., and Zhang, W. H. (2010) Phosphatidic acid mediates salt stress response by regulation of MPK6 in Arabidopsis thaliana. *New Phytol.* **188,** 762–773
13. Schmidt, R., Mieulet, D., Hubberten, H. M., Obata, T., Hoefgen, R., Fernie, A. R., Fisahn, J., Segundo, B. S., Guiderdoni, E., Schippers, J. H. M., and Mueller-Roeber, B. (2013) SALT-RESPONSIVE ERF1 regulates reactive oxygen species-dependent signaling during the initial response to salt stress in rice. *Plant Cell* **25,** 2115–2131
14. Latz, A., Mehlmer, N., Zapf, S., Mueller, T. D., Wurzinger, B., Pfister, B., Csaszar, E., Hedrich, R., Teige, M., and Becker, D. (2013) Salt stress triggers phosphorylation of the Arabidopsis vacuolar K channel TPK1 by calcium-dependent protein kinases (CDPKs). *Mol. Plant* **6,** 1274–1289
15. Lin, H. X., Yang, Y. Q., Quan, R. D., Mendoza, I., Wu, Y. S., Du, W. M., Zhao, S. S., Schumaker, K. S., Pardo, J. M., and Guo, Y. (2009) Phosphorylation of SOS3-LIKE CALCIUM BINDING PROTEIN8 by SOS2 protein kinase stabilizes their protein complex and regulates salt tolerance in Arabidopsis. *Plant cell* **21,** 1607–1619
16. Yan, J. H., Wang, B. A., Jiang, Y. N., Cheng, L. J., and Wu, T. L. (2014) GmFNSII-Controlled soybean flavone metabolism responds to abiotic stresses and regulates plant salt tolerance. *Plant Cell Physiol.* **55,** 74–86
17. Aghaei, K., Ehsanpour, A., Shah, A., and Komatsu, S. (2009) Proteome analysis of soybean hypocotyl and root under salt stress. *Amino Acids* **36,** 91–98
18. Toorchi, M., Yukawa, K., Nouri, M.-Z., and Komatsu, S. (2009) Proteomics approach for identifying osmotic-stress-related proteins in soybean roots. *Peptides* **30,** 2108–2117
19. Ge, Y., Li, Y., Zhu, Y.-M., Bai, X., Lv, D.-K., Guo, D., Ji, W., and Cai, H. (2010) Global transcriptome profiling of wild soybean (*Glycine soja*) roots under $NaHCO_3$ treatment. *BMC Plant Biol.* **10,** 153
20. Lu, Y., Lam, H., Pi, E., Zhan, Q., Tsai, S., Wang, C., Kwan, Y., and Ngai, S. (2013) Comparative metabolomics in *Glycine max* and *Glycine soja* under salt stress to reveal the phenotypes of their offspring. *J. Agr. Food Chem.* **61,** 8711–8721
21. Qin, J., Gu, F., Liu, D., Yin, C., Zhao, S., Chen, H., Zhang, J., Yang, C., Zhan, X., and Zhang, M. (2013) Proteomic analysis of elite soybean Jidou17 and its parents using iTRAQ-based quantitative approaches. *Proteome Sci.* **11,** 12
22. Ficarro, S. B., McCleland, M. L., Stukenberg, P. T., Burke, D. J., Ross, M. M., Shabanowitz, J., Hunt, D. F., and White, F. M. (2002) Phosphoproteome analysis by mass spectrometry and its application to Saccharomyces cerevisiae. *Nat Biotechnol* **20,** 301–305
23. Gruhler, A., Olsen, J. V., Mohammed, S., Mortensen, P., Færgeman, N. J., Mann, M., and Jensen, O. N. (2005) Quantitative phosphoproteomics applied to the yeast pheromone signaling pathway. *Mol. Cell. Proteomics* **4,** 310–327
24. Beausoleil, S. A., Jedrychowski, M., Schwartz, D., Elias, J. E., Villén, J., Li, J., Cohn, M. A., Cantley, L. C., and Gygi, S. P. (2004) Large-scale characterization of HeLa cell nuclear phosphoproteins. *Proc. Natl. Acad. Sci. U.S.A.* **101,** 12130–12135
25. Larsen, M. R., Thingholm, T. E., Jensen, O. N., Roepstorff, P., and Jørgensen, T. J. (2005) Highly selective enrichment of phosphorylated peptides from peptide mixtures using titanium dioxide microcolumns. *Mol. Cell. Proteomics* **4,** 873–886
26. Mazanek, M., Mituloviae, G., Herzog, F., Stingl, C., Hutchins, J. R., Peters, J. M., and Mechtler, K. (2007) Titanium dioxide as a chemo-affinity solid phase in offline phosphopeptide chromatography prior to HPLC-MS/MS analysis. *Nat. Protoc.* **2,** 1059–1069
27. Guan, R. X., Qu, Y., Guo, Y., Yu, L. L., Liu, Y., Jiang, J. H., Chen, J. G., Ren, Y. L., Liu, G. Y., Tian, L., Jin, L. G., Liu, Z. X., Hong, H. L., Chang, R. Z., Gilliham, M., and Qiu, L. J. (2014) Salinity tolerance in soybean is modulated by natural variation in *GmSALT3. Plant J.* **80,** 937–950
28. Yuan, C. P., Zhou, G., Li, Y. H., Wang, K. J., Wang, Z., Li, X. H., Chang, R. Z., Qiu, L. J. (2008) Cloning and sequence diversity analysis of *GmHs1*$^{pro-1}$ in Chinese domesticated and wild soybeans. *Mol Breeding* **22,** 593–602
29. Lv, D. W., Subburaj, S., Cao, M., Yan, X., Li, X. H., Appels, R., Sun, D. F., Ma, W. J., and Yan, Y. M. (2014) Proteome and phosphoproteome characterization reveals new response and defense mechanisms of *Brachypodium distachyon* leaves under salt stress. *Mol. Cell. Proteomics* **13,** 632–652
30. Kao, S. H., Wong, H. K., Chiang, C. Y., and Chen, H. M. (2008) Evaluating the compatibility of three colorimetric protein assays for two-dimensional electrophoresis experiments. *Proteomics* **8,** 2178–2184
31. Wisniewski, J. R., Zougman, A., and Mann, M. (2009) Combination of FASP and StageTip-based fractionation allows in-depth analysis of the hippocampal membrane proteome. *J. Proteome Res.* **8,** 5674–5678
32. Wisniewski, J. R., Zougman, A., Nagaraj, N., and Mann, M. (2009) Universal sample preparation method for proteome analysis. *Nat. Methods* **6,** 359-U360
33. Ostasiewicz, P., Zielinska, D. F., Mann, M., and Wisniewski, J. R. (2010) Proteome, phosphoproteome, and N-glycoproteome are quantitatively preserved in formalin-fixed paraffin-embedded tissue and analyzable by high-resolution mass spectrometry. *J. Proteome Res.* **9,** 3688–3700
34. Dong, M., Gu, J., Zhang, L., Chen, P., Liu, T., Deng, J., Lu, H., Han, L., and Zhao, B. (2014) Comparative proteomics analysis of superior and inferior spikelets in hybrid rice during grain filling and response of inferior spikelets to drought stress using isobaric tags for relative and absolute quantification. *J. Proteomics* **109,** 382–399
35. Cox, J., and Mann, M. (2008) MaxQuant enables high peptide identification rates, individualized p.p.b.-range mass accuracies and proteome-wide protein quantification. *Nat. Biotechnol* **26,** 1367–1372
36. Tran, H. N. N., Brechenmacher, L., Aldrich, J. T., Clauss, T. R., Gritsenko, M. A., Hixson, K. K., Libault, M., Tanaka, K., Yang, F., Yao, Q. M., Pasa-Tolic, L., Xu, D., Nguyen, H. T., and Stacey, G. (2012) Quantitative phosphoproteomic analysis of soybean root hairs inoculated with *Bradyrhizobium japonicum. Mol. Cell. Proteomics* **11,** 1140–1155
37. Jones, K. A., Kim, P. D., Patel, B. B., Kelsen, S. G., Braverman, A., Swinton, D. J., Gafken, P. R., Jones, L. A., Lane, W. S., Neveu, J. M., Leung, H. C., Shaffer, S. A., Leszyk, J. D., Stanley, B. A., Fox, T. E., Stanley, A., Hall, M. J., Hampel, H., South, C. D., de la Chapelle, A., Burt, R. W., Jones, D. A., Kopelovich, L., and Yeung, A. T. (2013) Immunodepletion plasma proteomics by tripleTOF 5600 and Orbitrap elite/LTQ-Orbitrap Velos/Q exactive mass spectrometers. *J. Proteome Res.* **12,** 4351–4365
38. Wang, G., Zeng, H., Hu, X., Zhu, Y., Chen, Y., Shen, C., Wang, H., Poovaiah, B. W., and Du, L. (2015) Identification and expression analyses of calmodulin-binding transcription activator genes in soybean. *Plant Soil* **386,** 205–221
39. Ye, J., Coulouris, G., Zaretskaya, I., Cutcutache, I., Rozen, S., and Madden,

T. L. (2012) Primer-BLAST: a tool to design target-specific primers for polymerase chain reaction. *BMC Bioinformatics* **13,** 134
40. Schwartz, D., and Gygi, S. P. (2005) An iterative statistical approach to the identification of protein phosphorylation motifs from large-scale data sets. *Nat. Biotechnol.* **23,** 1391–1398
41. Mathelier, A., Zhao, X. B., Zhang, A. W., Parcy, F., Worsley-Hunt, R., Arenillas, D. J., Buchman, S., Chen, C. Y., Chou, A., Ienasescu, H., Lim, J., Shyr, C., Tan, G., Zhou, M., Lenhard, B., Sandelin, A., and Wasserman, W. W. (2014) JASPAR 2014: an extensively expanded and updated open-access database of transcription factor binding profiles. *Nucleic Acids Res.* **42,** D142-D147
42. Bryne, J. C., Valen, E., Tang, M. H. E., Marstrand, T., Winther, O., da Piedade, I., Krogh, A., Lenhard, B., and Sandelin, A. (2008) JASPAR, the open access database of transcription factor-binding profiles: new content and tools in the 2008 update. *Nucleic Acids Res.* **36,** D102-D106
43. Zhang, Z., Pang, X., Xuewu, D., Ji, Z., and Jiang, Y. (2005) Role of peroxidase in anthocyanin degradation in litchi fruit pericarp. *Food Chem.* **90,** 47–52
44. Re, R., Pellegrini, N., Proteggente, A., Pannala, A., Yang, M., and Rice-Evans, C. (1999) Antioxidant activity applying an improved ABTS radical cation decolorization assay. *Free Radical Biol. Med.* **26,** 1231–1237
45. Qi, X. P., Li, M. W., Xie, M., Liu, X., Ni, M., Shao, G. H., Song, C., Yim, A. K. Y., Tao, Y., Wong, F. L., Isobe, S., Wong, C. F., Wong, K. S., Xu, C. Y., Li, C. Q., Wang, Y., Guan, R., Sun, F. M., Fan, G. Y., Xiao, Z. X., Zhou, F., Phang, T. H., Liu, X., Tong, S. W., Chan, T. F., Yiu, S. M., Tabata, S., Wang, J., Xu, X., and Lam, H. M. (2014) Identification of a novel salt tolerance gene in wild soybean by whole-genome sequencing. *Nat. Commun.* **5,** 4340–4350
46. Shi, H., Lee, B. H., Wu, S. J., and Zhu, J. K. (2003) Overexpression of a plasma membrane Na^+/H^+ antiporter gene improves salt tolerance in Arabidopsis thaliana. *Nat. Biotechnol.* **21,** 81–85
47. Dudonne, S., Vitrac, X., Coutiere, P., Woillez, M., and Mérillon, J.-M. (2009) Comparative study of antioxidant properties and total phenolic content of 30 plant extracts of industrial interest using DPPH, ABTS, FRAP, SOD, and ORAC assays. *J. Agr. Food Chem.* **57,** 1768–1774
48. Zulawski, M., Braginets, R., and Schulze, W. X. (2013) PhosPhAt goes kinases-searchable protein kinase target information in the plant phosphorylation site database PhosPhAt. *Nucleic Acids Res.* **41,** D1176-D1184
49. Huang, H. D., Lee, T. Y., Tzeng, S. W., and Horng, J. T. (2005) KinasePhos: a web tool for identifying protein kinase-specific phosphorylation sites. *Nucleic Acids Res.* **33,** W226–229
50. Broin, P. O., Smith, T. J., and Golden, A. (2015) Alignment-free clustering of transcription factor binding motifs using a genetic-k-medoids approach. *BMC Bioinformatics* **16,** 22
51. Matsuura, H., Ishibashi, Y., Shinmyo, A., Kanaya, S., and Kato, K. (2010) Genome-wide analyses of early translational responses to elevated temperature and high salinity in *Arabidopsis thaliana. Plant Cell Physiol.* **51,** 448–462
52. Wu, T., Pi, E.-X., Tsai, S.-N., Lam, H.-M., Sun, S.-M., Kwan, Y. W., and Ngai, S.-M. (2011) GmPHD5 acts as an important regulator for crosstalk between histone H3K4 di-methylation and H3K14 acetylation in response to salinity stress in soybean. *BMC Plant Biol.* **11,** 178
53. Sobhanian, H., Razavizadeh, R., Nanjo, Y., Ehsanpour, A. A., Jazii, F. R., Motamed, N., and Komatsu, S. (2010) Proteome analysis of soybean leaves, hypocotyls and roots under salt stress. *Proteome Sci.* **8,** 1–15
54. Chen, F., Li, B., Li, G., Charron, J. B., Dai, M., Shi, X., and Deng, X. W. (2014) Arabidopsis phytochrome a directly targets numerous promoters for individualized modulation of genes in a wide range of pathways. *Plant Cell* **26,** 1949–1966
55. Alimohammadi, M., de Silva, K., Ballu, C., Ali, N., and Khodakovskaya, M. V. (2012) Reduction of inositol (1,4,5)-trisphosphate affects the overall phosphoinositol pathway and leads to modifications in light signalling and secondary metabolism in tomato plants. *J. Exp. Bot.* **63,** 825–835
56. Wang, K. R., Senthil-Kumar, M., Ryu, C. M., Kang, L., and Mysore, K. S. (2012) Phytosterols play a key role in plant innate immunity against bacterial pathogens by regulating nutrient efflux into the apoplast. *Plant Physiol.* **158,** 1789–1802
57. O'Brien, M., Chantha, S. C., Rahier, A., and Matton, D. P. (2005) Lipid signaling in plants. Cloning and expression analysis of the obtusifoliol 14alpha-demethylase from *Solanum chacoense* Bitt., a pollination- and fertilization-induced gene with both obtusifoliol and lanosterol demethylase activity. *Plant Physiol.* **139,** 734–749
58. Zhu, J. K. (2003) Regulation of ion homeostasis under salt stress. *Curr. Opin. Plant Biol.* **6,** 441–445
59. Knight, H., Trewavas, A. J., and Knight, M. R. (1997) Calcium signalling in *Arabidopsis thaliana* responding to drought and salinity. *Plant J.* **12,** 1067–1078
60. Qiu, Q.-S., Guo, Y., Dietrich, M. A., Schumaker, K. S., and Zhu, J.-K. (2002) Regulation of SOS1, a plasma membrane Na^+/H^+ exchanger in *Arabidopsis thaliana*, by SOS2 and SOS3. *Proc. Natl. Acad. Sci. U.S.A.* **99,** 8436–8441
61. Wu, S.-J., Ding, L., and Zhu, J.-K. (1996) SOS1, a genetic locus essential for salt tolerance and potassium acquisition. *Plant Cell* **8,** 617–627
62. Kudla, J., Batistič, O., and Hashimoto, K. (2010) Calcium signals: the lead currency of plant information processing. *Plant Cell* **22,** 541–563
63. Curran, A., Chang, F., Chang, C.-L., Garg, S., Miguel, R. M., Barron, Y. D., Li, Y., Romanowsky, S., Cushman, J. C., and Gribskov, M. (2011) Calcium-dependent protein kinases from Arabidopsis show substrate specificity differences in an analysis of 103 substrates. *Frontiers Plant Sci.* **2,** 1–15
64. Hedrich, R., and Kudla, J. (2006) Calcium signaling networks channel plant K^+ uptake. *Cell* **125,** 1221–1223
65. Miller, G., Suzuki, N., CIFTCI-YILMAZ, S., and Mittler, R. (2010) Reactive oxygen species homeostasis and signalling during drought and salinity stresses. *Plant Cell Environ.* **33**, 453–467
66. Tognetti, V. B., Mühlenbock, P., and Van Breusegem, F. (2012) Stress homeostasis–the redox and auxin perspective. *Plant Cell Environ.* **35,** 321–333
67. Iglesias, M. J., Terrile, M. C., Bartoli, C. G., D'Ippólito, S., and Casalongué, C. A. (2010) Auxin signaling participates in the adaptative response against oxidative stress and salinity by interacting with redox metabolism in Arabidopsis. *Plant Mol. Biol.* **74,** 215–222
68. Jain, M., and Khurana, J. P. (2009) Transcript profiling reveals diverse roles of auxin-responsive genes during reproductive development and abiotic stress in rice. *FEBS J.* **276,** 3148–3162
69. Blomster, T., Salojärvi, J., Sipari, N., Brosché, M., Ahlfors, R., Keinänen, M., Overmyer, K., and Kangasjärvi, J. (2011) Apoplastic reactive oxygen species transiently decrease auxin signaling and cause stress-induced morphogenic response in Arabidopsis. *Plant Physiol.* **157,** 1866–1883
70. Nakagami, H., Pitzschke, A., and Hirt, H. (2005) Emerging MAP kinase pathways in plant stress signalling. *Trends Plant Sci.* **10,** 339–346
71. Ichimura, K., Mizoguchi, T., Yoshida, R., Yuasa, T., and Shinozaki, K. (2000) Various abiotic stresses rapidly activate Arabidopsis MAP kinases ATMPK4 and ATMPK6. *Plant J.* **24,** 655–665
72. Page, C. C., Moser, C. C., Chen, X., and Dutton, P. L. (1999) Natural engineering principles of electron tunnelling in biological oxidation-reduction. *Nature* **402,** 47–52
73. Brandt, U. (2006) Energy converting NADH: quinone oxidoreductase (complex I). *Annu. Rev. Biochem.* **75,** 69–92
74. Wang, J., Zhang, H., and Allen, R. D. (1999) Overexpression of an Arabidopsis peroxisomal ascorbate peroxidase gene in tobacco increases protection against oxidative stress. *Plant Cell Physiol.* **40,** 725–732
75. Lee, S.-H., Ahsan, N., Lee, K.-W., Kim, D.-H., Lee, D.-G., Kwak, S.-S., Kwon, S.-Y., Kim, T.-H., and Lee, B.-H. (2007) Simultaneous overexpression of both CuZn superoxide dismutase and ascorbate peroxidase in transgenic tall fescue plants confers increased tolerance to a wide range of abiotic stresses. *J. Plant Physiol.* **164,** 1626–1638
76. Yoshimura, K., Yabuta, Y., Ishikawa, T., and Shigeoka, S. (2000) Expression of spinach ascorbate peroxidase isoenzymes in response to oxidative stresses. *Plant Physiol.* **123,** 223–234
77. Allen, R. D. (1995) Dissection of oxidative stress tolerance using transgenic plants. *Plant Physiol.* **107,** 1049
78. Lu, Z., Liu, D., and Liu, S. (2007) Two rice cytosolic ascorbate peroxidases differentially improve salt tolerance in transgenic Arabidopsis. *Plant Cell Rep.* **26,** 1909–1917
79. O'Keefe, D. P., Tepperman, J. M., Dean, C., Leto, K. J., Erbes, D. L., and Odell, J. T. (1994) Plant expression of a bacterial cytochrome P450 that catalyzes activation of a sulfonylurea pro-herbicide. *Plant Physiol.* **105,** 473–482
80. Dixon, R. A. (2001) Natural products and plant disease resistance. *Nature*

411, 843–847
81. Weisshaar, B., and Jenkins, G. I. (1998) Phenylpropanoid biosynthesis and its regulation. *Curr. Opin. Plant Biol.* **1,** 251–257
82. Zhu, Y., Nomura, T., Xu, Y., Zhang, Y., Peng, Y., Mao, B., Hanada, A., Zhou, H., Wang, R., Li, P., Zhu, X., Mander, L. N., Kamiya, Y., Yamaguchi, S., and He, Z. (2006) ELONGATED UPPERMOST INTERNODE encodes a cytochrome P450 monooxygenase that epoxidizes gibberellins in a novel deactivation reaction in rice. *Plant Cell* **18,** 442–456
83. Mayer, M. J., Narbad, A., Parr, A. J., Parker, M. L., Walton, N. J., Mellon, F. A., and Michael, A. J. (2001) Rerouting the plant phenylpropanoid pathway by expression of a novel bacterial enoyl-CoA hydratase/lyase enzyme function. *Plant Cell* **13,** 1669–1682
84. Morita, H., Shimokawa, Y., Tanio, M., Kato, R., Noguchi, H., Sugio, S., Kohno, T., and Abe, I. (2010) A structure-based mechanism for benzalacetone synthase from *Rheum palmatum. Proc. Natl. Acad. Sci. U.S.A.* **107,** 669–673
85. Heller, W. (1986) Flavonoid biosynthesis, an overview. *Prog. Clin. Biol. Res.* **213,** 25–42
86. Pelletier, M. K., and Shirley, B. W. (1996) Analysis of flavanone 3-hydroxylase in Arabidopsis seedlings. Coordinate regulation with chalcone synthase and chalcone isomerase. *Plant Physiol.* **111,** 339–345
87. Hur, S., Newby, Z. E., and Bruice, T. C. (2004) Transition state stabilization by general acid catalysis, water expulsion, and enzyme reorganization in Medicago savita chalcone isomerase. *Proc. Natl. Acad. Sci. U.S.A.* **101,** 2730–2735
88. Arts, I. C., and Hollman, P. C. (2005) Polyphenols and disease risk in epidemiologic studies. *Am. J. Clin. Nutr.* **81**, 317S-325S
89. Hughes, D. A. (2005) Plant polyphenols: modifiers of immune function and risk of cardiovascular disease. *Nutrition* **21,** 422–423
90. Xue, Y., Zhang, Y., Cheng, D., Daddy, S., and He, Q. (2014) Genetically engineering *Synechocystis* sp. Pasteur Culture Collection 6803 for the sustainable production of the plant secondary metabolite *p*-coumaric acid. *Proc. Natl. Acad. Sci. U.S.A.* **111,** 9449–9454
91. Yan, Y., Kohli, A., and Koffas, M. A. (2005) Biosynthesis of natural flavanones in *Saccharomyces cerevisiae. Appl. Environ Microb.* **71,** 5610–5613
92. Chen, L. J., Guo, H. M., Lin, Y., and Cheng, H. M. (2015) Chalcone synthase EaCHS1 from *Eupatorium adenophorum* functions in salt stress tolerance in tobacco. *Plant Cell Rep.* **34,** 885–894
93. Wang, H., Hu, T. J., Huang, J. Z., Lu, X., Huang, B. Q., and Zheng, Y. Z. (2013) The expression of *Millettia pinnata* chalcone isomerase in *Saccharomyces cerevisiae* salt-sensitive mutants enhances salt-tolerance. *Int. J. Mol. Sci.* **14,** 8775–8786
94. Mao, G., Seebeck, T., Schrenker, D., and Yu, O. (2013) CYP709B3, a cytochrome P450 monooxygenase gene involved in salt tolerance in *Arabidopsis thaliana. BMC Plant Biol.* **13,** 169
95. Stracke, R., Ishihara, H., Huep, G., Barsch, A., Mehrtens, F., Niehaus, K., and Weisshaar, B. (2007) Differential regulation of closely related R2R3-MYB transcription factors controls flavonol accumulation in different parts of the *Arabidopsis thaliana* seedling. *Plant J.* **50,** 660–677
96. Liao, Y., Zou, H. F., Wang, H. W., Zhang, W. K., Ma, B., Zhang, J. S., and Chen, S. Y. (2008) Soybean GmMYB76, GmMYB92, and GmMYB177 genes confer stress tolerance in transgenic Arabidopsis plants. *Cell Res.* **18,** 1047–1060
97. Du, H., Wang, Y. B., Xie, Y., Liang, Z., Jiang, S. J., Zhang, S. S., Huang, Y. B., and Tang, Y. X. (2013) Genome-wide identification and evolutionary and expression analyses of MYB-related genes in land plants. *DNA Res.* **20,** 437–448
98. Lafuente, A., Perez-Palacios, P., Doukkali, B., Molina-Sanchez, M. D., Jimenez-Zurdo, J. I., Caviedes, M. A., Rodriguez-Llorente, I. D., and Pajuelo, E. (2015) Unraveling the effect of arsenic on the model Medicago-Ensifer interaction: a transcriptomic meta-analysis. *New Phytol.* **205,** 255–272
99. Hellmann, H., Funck, D., Rentsch, D., and Frommer, W. B. (2000) Hypersensitivity of an Arabidopsis sugar signaling mutant toward exogenous proline application. *Plant Physiol.* **122,** 357–368
100. Hellmann, H., Funck, D., Rentsch, D., and Frommer, W. B. (2000) Hypersensitivity of an Arabidopsis sugar signaling mutant toward exogenous proline application. *Plant Physiol.* **123,** 779–789